

---

# Cascaded Learned Bloom Filter for Optimal Model-Filter Size Balance and Fast Rejection

---

Atsuki Sato<sup>\*1</sup> Yusuke Matsui<sup>\*1</sup>

## Abstract

Recent studies have demonstrated that learned Bloom filters, which combine machine learning with the classical Bloom filter, can achieve superior memory efficiency. However, existing learned Bloom filters face two critical unresolved challenges: the balance between the machine learning model size and the Bloom filter size is not optimal, and the reject time cannot be minimized effectively. We propose the Cascaded Learned Bloom Filter (CLBF) to address these issues. Our dynamic programming-based optimization automatically selects configurations that achieve an optimal balance between the model and filter sizes while minimizing reject time. Experiments on real-world datasets show that CLBF reduces memory usage by up to 24% and decreases reject time by up to 14 times compared to state-of-the-art learned Bloom filters.

## 1. Introduction

Bloom filters (Bloom, 1970) are ubiquitous data structures used for approximate membership queries. A Bloom filter compresses a set  $S$  into a bit array, enabling rapid determination of whether a query  $q$  is a *key* (i.e., an element included in  $S$ ) or a *non-key* (i.e., an element not included in  $S$ ). While a Bloom filter may misidentify a non-key as a key (false positive), it never misidentifies a key as a non-key (false negative). Due to their high memory efficiency, fast query performance, and the absence of false negatives, Bloom filters are widely employed in memory-constrained and latency-sensitive applications (Broder & Mitzenmacher, 2004; Chang et al., 2008). Recently, a new class of Bloom filters called Learned Bloom Filters (LBFs) has been proposed (Kraska et al., 2018). LBFs leverage a machine learning model to predict whether an input belongs to the set  $S$ , achieving superior memory efficiency compared to clas-

sical Bloom filters. Despite numerous attempts to further improve memory efficiency (Mitzenmacher, 2018; Dai & Shrivastava, 2020), existing LBFs face two critical unresolved issues: (1) the balance between the machine learning model size and the Bloom filter size remains suboptimal, and (2) the reject time cannot be effectively minimized.

**(1) The Balance Between Machine Learning Model Size and Bloom Filter Size:** Existing LBFs lack mechanisms to automatically balance the sizes of the machine learning model and the Bloom filters. An LBF consists of a machine learning model and one or more Bloom filters, aiming to minimize the total memory usage, i.e., the sum of the memory consumed by the machine learning model and the Bloom filters. Since a smaller machine learning model often—but not always—has lower accuracy, larger Bloom filters are needed to maintain the overall false positive rate of an LBF, whereas a larger model often—but not always—allows for smaller Bloom filters. Thus, it is a challenging task to strike a balance between the sizes of the machine learning model and the Bloom filters in LBFs, and to minimize the overall memory consumption. Existing LBF construction methods focus on optimizing the configuration of Bloom filters for a fixed, pre-trained model, without addressing the interplay between the sizes of the model and the Bloom filters.

**(2) The Reject Time:** Existing approaches do not provide automatic methods for minimizing reject time in LBFs. The short *reject time* of a Bloom filter (i.e., the time it takes to answer “ $q$  does not belong to  $S$ ”) is a key property and often more critical than the *accept time* (i.e., the time it takes to answer “ $q$  belongs to  $S$ ”). For example, consider using a Bloom filter as a pre-filter before performing **strict** membership queries in a large-scale key-value store or a database system. In such systems, checking whether a key exists often requires an expensive lookup operation, such as searching a B-tree, querying a distributed hash table, or accessing disk storage. The Bloom filter can pre-filter the majority of non-key queries at the cost of a small overhead. Let  $T$  denote the time required to perform a naive strict membership check without a pre-filter. Let  $f$  represent the Bloom filter’s false positive rate, and let  $t_a$  and  $t_r$  denote its accept and reject times, respectively. The response time for key queries is  $t_a + T$ , but since  $t_a \ll T$ , this is almost

---

<sup>\*</sup>Equal contribution <sup>1</sup>Graduate School of Information Science and Technology, The University of Tokyo, Tokyo, Japan. Correspondence to: Atsuki Sato <a\_sato@hal.t.u-tokyo.ac.jp>.

equivalent to  $T$ . On the other hand, the expected response time for non-key queries is given by:

$$(1 - f)t_r + f(t_a + T) \approx t_r + fT, \quad (1)$$

since  $t_a \ll T$  and  $f \ll 1$ . The expected reject time,  $t_r + fT$ , is significantly smaller than  $T$  when  $t_r$  and  $f$  are sufficiently small, highlighting the advantage of using a Bloom filter. As shown in Equation (1), reducing the reject time  $t_r$  is as important as minimizing the false positive rate  $f$ . However, most existing LBF research (Kraska et al., 2018; Mitzenmacher, 2018; Vaidya et al., 2021) focuses primarily on accuracy. While some studies (Fumagalli et al., 2022; Malchiodi et al., 2024) address reject time, they offer only heuristic guidelines and lack automatic methods for minimizing reject time.

To address these issues, we propose a novel learned Bloom filter with a cascaded structure called Cascaded Learned Bloom Filter (CLBF). CLBF offers two key features: (1) CLBF achieves an optimal balance of memory usage by training a larger machine learning model and then appropriately reducing its size, and (2) CLBF enables faster rejections through branching based on tentative outputs from the machine learning model and the intermediate Bloom filters. We can set the hyperparameters to control the trade-off between memory efficiency and reject time. Our optimization approach, based on dynamic programming, automatically adjusts CLBF to the optimal configuration for the given hyperparameter. Our experiments demonstrate that (1) CLBF reduces memory usage by up to 24% and (2) reject time by up to 14 times compared to the Partitioned Learned Bloom Filter (PLBF) (Vaidya et al., 2021), the state-of-the-art LBF.

## 2. Related Work

Bloom filter (Bloom, 1970) is one of the most fundamental and widely used data structures for approximate membership queries. Bloom filters can quickly respond to queries by only performing a few hash function evaluations and checking a few bits. Although Bloom filters may return false positives, they never yield false negatives. This property makes Bloom filters valuable in memory-constrained and latency-sensitive scenarios such as networks (Broder & Mitzenmacher, 2004; Tarkoma et al., 2011; Geravand & Ahmadi, 2013) and databases (Chang et al., 2008; Goodrich & Mitzenmacher, 2011; Lu et al., 2012). The parameters of a Bloom filter, such as the length of the bit array and the number of hash functions, are determined by the number of keys to store and the target false positive rate. Specifically, for a Bloom filter storing  $n$  keys with a false positive rate  $\varepsilon$ , the required bit array length is  $\log_2(e) \cdot n \log_2(1/\varepsilon)$ , which is  $\log_2(e)$  times the theoretical lower bound of  $n \log_2(1/\varepsilon)$  (Pagh et al., 2005). Several improved versions of the Bloom filter, such as the Cuckoo filter (Fan et al.,

2014), Vacuum filter (Wang & Zhou, 2019), Xor filter (Graf & Lemire, 2020), and Ribbon filter (Dillinger & Walzer, 2021), have been proposed to get closer to the theoretical lower bound.

Recently, the concept of Learned Bloom Filter (LBF), which enhances the memory efficiency of Bloom filters using machine learning models, was introduced (Kraska et al., 2018). They proposed an LBF that uses a machine learning model, which predicts whether the input is included in the set  $S$ , as a pre-filter before a classical Bloom filter (Figure 1(a)). In this LBF, elements predicted by the model as included in the set  $S$  are not inserted into the classical Bloom filter, while those predicted as not included are. When this LBF answers a query, it immediately answers  $q \in S$  if the model predicts the query is in the set. In contrast, if the model predicts the query is not in the set, this LBF uses the classical Bloom filter. This design reduces the number of elements stored in the Bloom filter, thus reducing the total memory usage.

Numerous subsequent studies have sought to improve this structure further. Sandwiched LBF (Mitzenmacher, 2018) sandwiches the machine learning model with two Bloom filters (Figure 1(b)). It is demonstrated that the memory efficiency is further improved by optimizing the size of the two Bloom filters. Ada-BF (Dai & Shrivastava, 2020) and PLBF (Vaidya et al., 2021) further enhance memory efficiency by utilizing the *score*, which is the prediction of the machine learning model regarding the likelihood that an input element is included in the set (Figure 1(c)). These LBFs employ multiple Bloom filters with different false positive rates, selecting the appropriate filter based on the score. This approach allows for a more continuous and fine-grained utilization of the model predictions.

While most research on LBFs has focused on the optimal configuration of Bloom filters for a fixed trained machine learning model, some studies have investigated the choice of the machine learning model itself (Fumagalli et al., 2022; Dai et al., 2022; Malchiodi et al., 2024). These studies evaluate various machine learning models and LBF configuration methods (such as sandwiched LBF and PLBF) across different datasets, measuring memory efficiency and reject times. The results suggest that the optimal machine learning model varies depending on dataset noisiness, ease of learning, and the importance of minimizing reject time. However, these studies provide only general guidelines based on observed trends, and no method has yet been proposed for automatically selecting the optimal machine learning model.

Optimizing the hash functions is another approach to improving the memory efficiency. Hash Adaptive Bloom Filter (HABF) (Xie et al., 2021b) uses a lightweight data structure called HashExpressor to select suitable hash functions for each key, and Projection Hash Bloom Filter (PHBF) (Bhattacharya et al., 2022a) employs projections as hash functions.

Unlike LBFs, these approaches avoid classifier training and instead pack information into a lighter structure.

### 3. Method: Cascaded Learned Bloom Filter

This section describes the architecture and construction of our proposed Cascaded Learned Bloom Filter (CLBF). In Section 3.1, we describe the architecture of CLBF. Then, we formulate the problem of constructing CLBF in Section 3.2, and the optimization method for configuring CLBF using dynamic programming is described in Section 3.3.

#### 3.1. Architectural Design and Workflow

CLBF employs a cascade structure consisting of multiple machine learning models and multiple Bloom filters arranged alternately (Figure 2). Any machine learning model can be used, including very simple ones. In fact, in our experiments, each machine learning model in CLBF corresponds to each weak learner trained with a boosting algorithm (as detailed in Section 4). By optimizing the number of machine learning models (weak learners) and the false positive rate of each bloom filter, CLBF not only balances model and filter sizes but also shortens the reject time.

CLBF processes a query  $q$  as follows: The query first enters the initial *Trunk Bloom filter*  $TBF_1$ . If  $TBF_1$  determines  $q \notin \mathcal{S}$ , CLBF immediately returns  $q \notin \mathcal{S}$ . Otherwise, the query is passed to the first machine learning model,  $ML_1$ , which outputs a score indicating the likelihood that  $q$  is in  $\mathcal{S}$ . If the score exceeds threshold  $\theta_1$ , the initial *Branch Bloom filter*  $BBF_1$  makes the final determination. Otherwise,  $q$  is passed to the next Trunk Bloom filter,  $TBF_2$ . In this way, CLBF alternates between branching based on the score and filtering using Bloom filters. When the query reaches the  $D$ -th (i.e., final) machine learning model, CLBF adopts the same approach as PLBF; multiple thresholds are set, and based on the range in which the query score falls, one of the  $K$  *Final Bloom filters* ( $FBF_1, FBF_2, \dots, FBF_K$ ) is used for the final determination. When inserting a key into CLBF, the key is inserted into **all** Bloom filters traversed by the process outlined above, ensuring the absence of false negatives. The exact algorithms for key insertion and query responses are detailed in Appendix A.1.

Here, we emphasize that the CLBF architecture generalizes existing LBF architectures (Figures 1 and 2) and that our optimization method can identify the optimal configuration within this unified framework. For example, a CLBF with only one Trunk Bloom filter and one Final Bloom filter is equivalent to a sandwiched LBF, and a CLBF that omits both Trunk and Branch Bloom filters while employing multiple Final Bloom filters is equivalent to a PLBF. Within this generalized framework, we address more general and flexible optimization problems than those addressed by existing

LBFs; Our construction method optimizes the number of machine learning models, taking into account the reject time. As a result, CLBF achieves superior memory efficiency and shorter reject time compared to existing LBFs.

The notations for CLBF description are as follows (most of the variables defined here are illustrated in Figure 2):  $D$  denotes the number of machine learning models CLBF uses (we optimize  $D$  using dynamic programming). The false positive rate of  $TBF_d$  ( $d = 1, 2, \dots, D$ ),  $BBF_d$  ( $d = 1, 2, \dots, D - 1$ ), and  $FBF_k$  ( $k = 1, 2, \dots, K$ ) are denoted by  $f_d^{(t)}$ ,  $f_d^{(b)}$ , and  $f_k^{(f)}$ , respectively. These false positive rates can also be expressed as vectors, e.g.,  $\mathbf{f}^{(t)} = [f_1^{(t)}, f_2^{(t)}, \dots, f_D^{(t)}]$ . Additionally, we collectively refer to these vectors as  $\mathcal{F} = \{\mathbf{f}^{(t)}, \mathbf{f}^{(b)}, \mathbf{f}^{(f)}\}$  for convenience.  $\text{Size}(\cdot)$  and  $\text{Time}(\cdot)$  represent the memory size and the inference time of the input, respectively, e.g.,  $\text{Size}(ML_d)$  represents the memory size of  $ML_d$ .  $\mathcal{S}$  represents the set stored by CLBF, and  $n$  denotes the number of elements in  $\mathcal{S}$ .  $\mathcal{Q}$  refers to the non-key set used for construction of CLBF.

#### 3.2. Problem Formulation

The goal of CLBF construction is to minimize the weighted sum of memory usage and the expected reject time, subject to an accuracy constraint. Here, we provide a detailed explanation of the components required for CLBF construction, the parameters to be optimized, and the objective function to be minimized.

**Requirements for CLBF Construction.** To construct the CLBF, the user must provide the following components: several pre-trained machine learning models, two hyperparameters, and validation data. The machine learning models are trained to perform binary classification between key and non-key using the sets  $\mathcal{S}$  and  $\mathcal{Q}$  (or their subsets). The number of pre-trained models is denoted by  $\bar{D}$ . Among these pre-trained models  $ML_1, ML_2, \dots, ML_{\bar{D}}$ , only the first  $D$  ( $\leq \bar{D}$ ) models, i.e.,  $ML_1, ML_2, \dots, ML_D$ , are used in the CLBF. The value of  $D$  is optimized during CLBF construction. The two hyperparameters are  $F$  ( $\in (0, 1)$ ), which represents the target false positive rate for the CLBF, and  $\lambda$  ( $\in [0, 1]$ ), which controls the trade-off between memory efficiency and reject time. The CLBF is optimized to minimize memory usage and reject time, subject to the constraint that the expected false positive rate does not exceed  $F$ . As  $\lambda$  increases, greater emphasis is placed on memory efficiency; specifically, when  $\lambda = 1$ , only memory usage is minimized, while when  $\lambda = 0$ , only reject time is minimized.

**Parameters to be Optimized.** In the construction of CLBF, the parameters  $D$  and  $\mathcal{F} (= \{\mathbf{f}^{(t)}, \mathbf{f}^{(b)}, \mathbf{f}^{(f)}\})$  are optimized. Another parameter,  $\theta_d$  ( $d = 1, \dots, D - 1$ ), i.e., the threshold for branching based on the tentative score out-

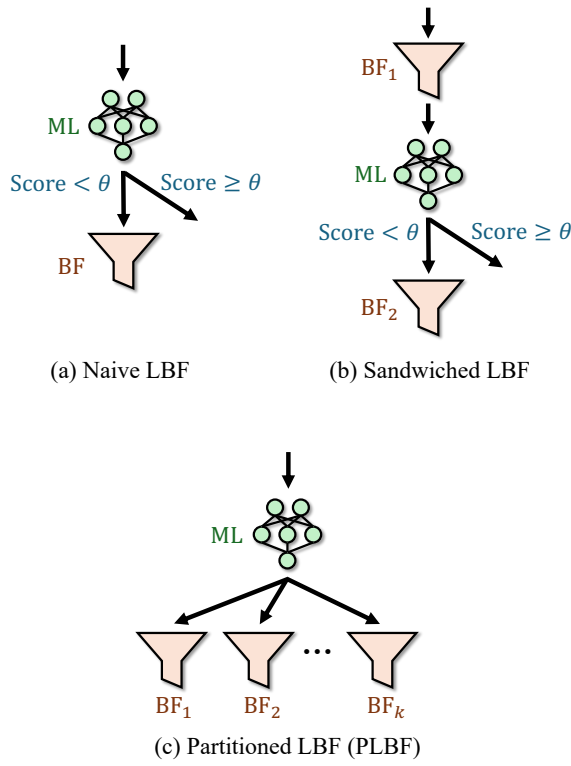


Figure 1: The architecture of Existing LBFs: (a) Naive LBF (Kraska et al., 2018) has a single backup Bloom filter. (b) Sandwiched LBF (Mitzenmacher, 2018) applies a pre-filter before the model inference. (c) PLBF (Vaidya et al., 2021) uses multiple backup Bloom filters.

put by  $ML_d$ , should also be optimized. However, jointly optimizing  $\theta_d$  with the other parameters is too challenging, as the value of  $\theta_d$  affects the score distributions output by  $ML_{d+1}$  and subsequent models, and capturing these effects is difficult. Thus, we adopt a heuristic approach, evaluating several candidates  $\theta$  ( $= [\theta_1, \theta_2, \dots, \theta_{D-1}]$ ) and selecting the one that minimizes the objective function. Specifically, for each  $\alpha$  ( $\in \{0.5, 0.2, 0.1, \dots, 0.0001, 0.0\}$ ), we evaluate  $\theta$  such that  $\theta_d$  is the top- $\alpha$  (ratio) score of non-keys output by  $ML_d$ . For the final machine learning model,  $ML_D$ , the thresholds are set to maximize the KL divergence between the score distributions of keys and non-keys, following the same method as in the PLBF (Vaidya et al., 2021).

Once the thresholds are fixed, we can measure the proportion of keys and non-keys passed to each Bloom filter and machine learning model using the validation data. In this measurement, filtering using TBFs is **not** performed; only the branching based on the tentative outputs of the machine

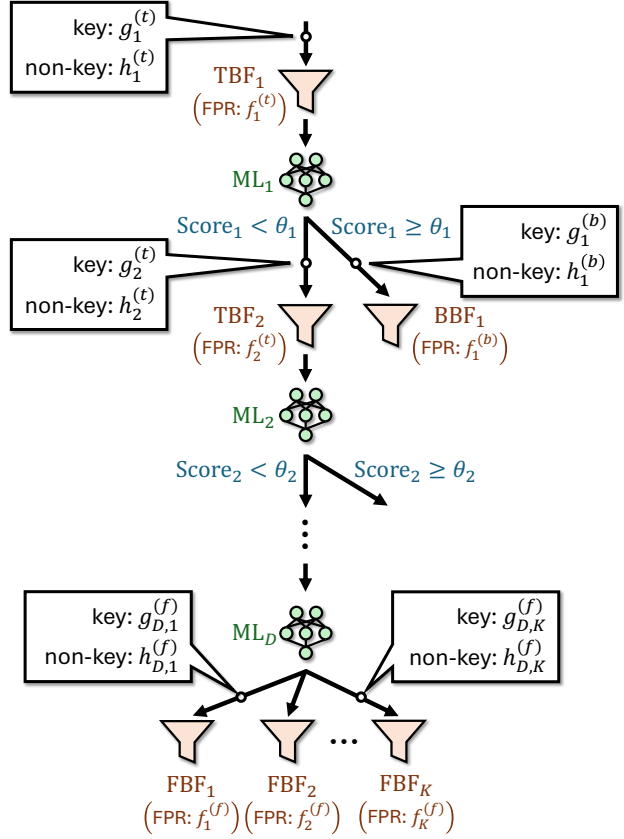


Figure 2: The architecture of CLBF: CLBF alternates between score-based branching and Bloom filter-based filtering. This design generalizes the architectures of sandwiched LBF and PLBF. Note that  $g_*^{(*)}$  and  $h_*^{(*)}$  represent the proportions of keys and non-keys passing through each root when filtering using TBFs is **not** performed.

learning models are applied. We define  $g_d^{(t)}$  and  $h_d^{(t)}$  as the proportions of keys and non-keys in the validation data that are passed to  $TBF_d$ , respectively. Similarly, we define  $g_d^{(b)}$  and  $h_d^{(b)}$  as the proportions of keys and non-keys that are passed to  $BBF_d$ . Finally, we define  $g_{D,k}^{(f)}$  and  $h_{D,k}^{(f)}$  as the proportions of keys and non-keys passed to  $FBF_k$ .

**Objective Function and Constraint.** The following objective function is minimized under the constraint that the “expected” false positive rate does not exceed  $F$ :

$$\lambda \cdot \frac{M(D, \mathcal{F})}{M_{BF}} + (1 - \lambda) \cdot \frac{R(D, \mathcal{F})}{R_{BF}}, \quad (2)$$

where  $M(D, \mathcal{F})$  represents the memory usage of the CLBF, and  $R(D, \mathcal{F})$  denotes the “expected” reject time. The expected false positive rate and the expected reject time are calculated using the validation data. The constants  $M_{BF}$  and  $R_{BF}$  are scaling factors to align the units of the two

terms, with  $M_{\text{BF}}$  representing the memory usage and  $R_{\text{BF}}$  representing the reject time of a standard classical Bloom filter under the same settings of the number of keys  $n$  and the false positive rate  $F$ . These constants are measured using the validation data: we construct a Bloom filter with  $F$  false positive rate that stores  $n$  keys, then measure the average reject time by repeatedly querying for non-keys.  $M(D, \mathcal{F})$  and  $R(D, \mathcal{F})$  can be written as follows:

$$M(D, \mathcal{F}) = \sum_{i=1}^D \text{Size}(\text{ML}_i) + \sum_{i=1}^D \text{Size}(\text{TBF}_i) + \sum_{i=1}^{D-1} \text{Size}(\text{BBF}_i) + \sum_{k=1}^K \text{Size}(\text{FBF}_k), \quad (3)$$

$$R(D, \mathcal{F}) = \sum_{i=1}^D \left( \text{Time}(\text{ML}_i) \cdot h_i^{(t)} \prod_{j=1}^i f_j^{(t)} \right). \quad (4)$$

In Equation (4), it is assumed that the reject time can be approximated by the total time taken by the inference of the machine learning models.  $\text{Time}(\text{ML}_i)$  is a constant obtained by performing several inference runs and averaging the observed inference times.

Here, we provide a detailed explanation of the factor  $h_i^{(t)} \prod_{j=1}^i f_j^{(t)}$  appearing in Equation (4). This factor represents the expected proportion of non-key queries processed by  $\text{ML}_i$ . Recall that  $h_i^{(t)}$  denotes the proportion of non-key queries reaching  $\text{ML}_i$  when no filtering is applied by the TBFs. Taking into account the filtering by  $\text{TBF}_1$ , which has a false positive rate of  $f_1^{(t)}$ , the expected proportion of non-key queries reaching  $\text{ML}_1$  is  $h_1^{(t)} f_1^{(t)}$ . This is because only non-keys queries that pass through  $\text{TBF}_1$  as false positives reach  $\text{ML}_1$ . Similarly, the expected proportion of non-key queries reaching  $\text{ML}_2$  is  $h_2^{(t)} \prod_{j=1}^2 f_j^{(t)}$ , because non-key queries that pass through both  $\text{TBF}_1$  and  $\text{TBF}_2$  as false positives reach  $\text{ML}_2$ . In this way, we can conclude that the proportion of non-key queries processed by  $\text{ML}_i$  is given by  $h_i^{(t)} \prod_{j=1}^i f_j^{(t)}$ .

### 3.3. Dynamic Programming for CLBF Construction

Here, we introduce a dynamic programming method to determine the parameters that minimize the objective function given in Equation (2). This dynamic programming method obtains the optimal configuration by repeating the following process in order of  $d = \bar{D} - 1, \bar{D} - 2, \dots, 1$ : based on the information of the optimal configuration at depth  $d + 1$ , make the optimal choice at depth  $d$  of whether to use FBFs (Figure 3a) or to perform branching (Figure 3b). By repeating this process recursively up to  $d = 1$ , we can identify the overall optimal configuration of the CLBF. In this process, the factor  $\prod_{j=1}^d f_j^{(t)}$  plays a critical role. As detailed in

the previous section, the proportion of non-key queries processed by  $\text{ML}_d$  is given by  $h_d^{(t)} \prod_{j=1}^d f_j^{(t)}$ . Similarly, the proportion of non-keys handled by components below  $\text{ML}_d$  (e.g.,  $\text{TBF}_{d+1}$ ,  $\text{BBF}_d$ , and FBFs) is also proportional to  $\prod_{j=1}^d f_j^{(t)}$ . Therefore, the dynamic programming function we define below,  $\text{dp}(d, T)$ , takes as inputs not only  $d$  but also  $T$ , where  $T = \prod_{j=1}^{d-1} f_j^{(t)}$ .

Now, we describe the essence of our dynamic programming method using mathematical formulas (detailed explanations are given in Appendix A.2). The function  $\text{dp}(d, T) : \{1, 2, \dots, \bar{D}\} \times (0, 1] \rightarrow \mathbb{R}$  is defined intuitively as the minimum value of the objective function under  $\text{TBF}_d$ , subject to the constraint that  $\prod_{j=1}^{d-1} f_j^{(t)} = T$ . More precisely,  $\text{dp}(d, T)$  is defined as the solution to the following optimization problem:

$$\min_{D, \mathcal{F}} \left( \lambda \cdot \frac{M_d(D, \mathcal{F})}{M_{\text{BF}}} + (1 - \lambda) \cdot \frac{R_d(D, \mathcal{F})}{R_{\text{BF}}} \right) \quad (5)$$

$$\text{s.t. } \prod_{j=1}^{d-1} f_j^{(t)} = T, \quad (6)$$

where  $M_d(D, \mathcal{F})$  is defined as

$$M_d(D, \mathcal{F}) = \sum_{i=d}^D \text{Size}(\text{ML}_i) + \sum_{i=d}^D \text{Size}(\text{TBF}_i) + \sum_{i=d}^{D-1} \text{Size}(\text{BBF}_i) + \sum_{k=1}^K \text{Size}(\text{FBF}_k), \quad (7)$$

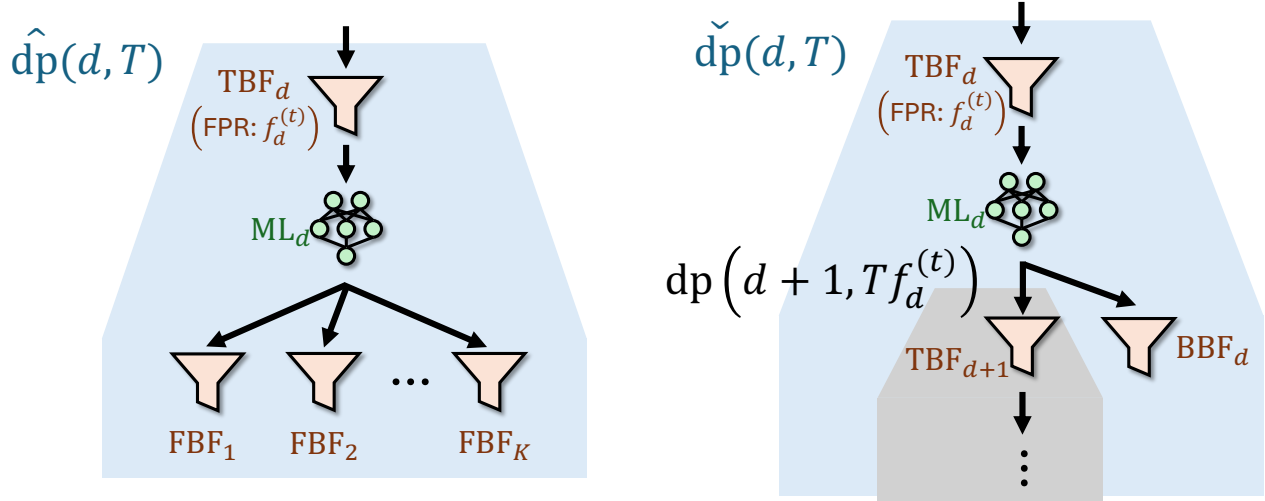
and  $R_d(D, \mathcal{F})$  is defined as

$$R_d(D, \mathcal{F}) = \sum_{i=d}^D \left( \text{Time}(\text{ML}_i) \cdot h_i^{(t)} \prod_{j=1}^i f_j^{(t)} \right). \quad (8)$$

By substituting  $d = 1, T = 1$  into Equations (5) and (6), we can see that  $\text{dp}(1, 1)$  is equivalent to the minimum value of Equation (2) because the constraint  $\prod_{j=1}^{d-1} f_j^{(t)} = T$  is no longer in effect and the objective function in Equation (5) is the same as Equation (2) when  $d = 1$  and  $T = 1$ .

We calculate  $\text{dp}(d, T)$  recursively by evaluating two distinct cases and select the better one: (1)  $D = d$ , where the immediate children of  $\text{ML}_d$  are FBFs (Figure 3a), and (2)  $D > d$ , where the two-way branching is performed directly under the  $\text{ML}_d$  (Figure 3b). We define  $\hat{\text{dp}}(d, T)$  as the solution to the optimization problem (Equations (5) and (6)) under the additional constraint  $D = d$ . Similarly, we define  $\check{\text{dp}}(d, T)$  as the solution under the additional constraint  $D > d$ . Then, we can compute  $\text{dp}(d, T)$  as follows:

$$\text{dp}(d, T) = \begin{cases} \hat{\text{dp}}(d, T) & d = \bar{D}, \\ \min(\hat{\text{dp}}(d, T), \check{\text{dp}}(d, T)) & \text{(else)}. \end{cases} \quad (9)$$



(a)  $\hat{\text{dp}}(d, T)$  is the minimum objective function value under  $\text{TBF}_d$  subject to the constraint that  $\prod_{j=1}^{d-1} f_j^{(t)} = T$  and  $D = d$ .

(b)  $\check{\text{dp}}(d, T)$  is the minimum objective function value under  $\text{TBF}_d$  subject to the constraint that  $\prod_{j=1}^{d-1} f_j^{(t)} = T$  and  $D > d$ .

Figure 3: The value of  $\text{dp}(d, T)$  is calculated by selecting the appropriate value from the case where  $D = d$ , i.e.,  $\hat{\text{dp}}(d, T)$ , and the case where  $D > d$ , i.e.,  $\check{\text{dp}}(d, T)$ . The value of  $\text{dp}(d+1, T f_d^{(t)})$  is used recursively to calculate  $\check{\text{dp}}(d, T)$ .

Note that when  $d = \bar{D}$ , the second case  $\check{\text{dp}}(d, T)$  is not evaluated because the number of machine learning models given is  $\bar{D}$ , and no further branching is possible.

We can (approximately) compute the values of  $\hat{\text{dp}}(d, T)$  because  $T = \prod_{j=1}^{d-1} f_j^{(t)}$  provides sufficient information to determine the configuration at depth  $d$  (Figure 3a). For a fixed  $f_d^{(t)}$ , i.e., the false positive rate of  $\text{TBF}_d$ , the expected proportions of keys and non-keys reaching each  $\text{FBF}$  can be determined. Thus, we can find the optimal false positive rate of each  $\text{FBF}$  using the method in PLBF (Vaidya et al., 2021) (please refer to Appendix A.2 for a detailed explanation). Although  $f_d^{(t)}$  can take any real value in  $(0, 1]$ , optimizing it in this continuous space is challenging. To address this, we evaluate  $f_d^{(t)}$  over a finite set of values,  $f_d^{(t)} \in \{p^0, p^1, \dots, p^{P-1}\}$ , for constants  $p \in (0, 1)$  and  $P \in \mathbb{N}$  (in our experiment, we set  $p = 0.5, P = 20$ ). For each candidate  $f_d^{(t)}$ , we compute the optimal false positive rates for the  $\text{FBFs}$ , evaluate the objective function in Equation (5), and then select the candidate that yields the smallest objective value to determine  $\hat{\text{dp}}(d, T)$ .

We can also calculate the value of  $\check{\text{dp}}(d, T)$  approximately in a similar way. For  $\text{BBF}_d$ , we can compute the optimal false positive rate using the PLBF method, just as we do when calculating  $\hat{\text{dp}}$ . For  $\text{TBF}_{d+1}$  and deeper parts, we can determine the optimal configurations using  $\text{dp}(d+1, T f_d^{(t)})$ . This is because, by the definition of  $\text{dp}$ ,  $\text{dp}(d+1, T f_d^{(t)})$  represents the objective function for  $\text{TBF}_{d+1}$  and deeper parts when they are optimally configured under the constraint

$\prod_{j=1}^d f_j^{(t)} = T f_d^{(t)}$ . Since  $T = \prod_{j=1}^{d-1} f_j^{(t)}$ , the constraint is satisfied, allowing us to use  $\text{dp}(d+1, T f_d^{(t)})$  to select the optimal configurations for  $\text{TBF}_{d+1}$  and deeper parts.

Using the dynamic programming approach described above, we can efficiently tackle a more complex problem than those addressed in existing research. Specifically, our setting introduces two additional challenges: the number of machine learning models is variable, and the expected reject time is explicitly considered. With appropriate implementation, the computational complexity of this dynamic programming approach becomes  $\mathcal{O}(\bar{D}P^2 + \bar{D}PK)$  (see Appendix A.2 for details). Since  $\bar{D}$ ,  $P$ , and  $K$  are typically no more than 100, the computation is sufficiently fast.

## 4. Experiments

In this section, we evaluate the memory efficiency and reject time of CLBF by comparing it with a standard Bloom filter and existing LBFs. The memory usage of LBFs is calculated as the sum of the memory consumed by the machine learning model and the Bloom filters within it. Here, training data refers to the data used for training the machine learning model, validation data refers to the data used for configuring the LBF, and test data refers to the data used to measure the accuracy and reject time of the Bloom filters. We conducted experiments using the following two datasets:

**Malicious URLs Dataset:** Following the previous studies on LBFs (Dai & Shrivastava, 2020; Vaidya et al., 2021), we used the Malicious URLs dataset (Siddhartha, 2021).

This dataset contains 223,088 malicious URLs and 428,103 benign URLs. The set of all malicious URLs constitutes the set  $\mathcal{S}$ , which the Bloom filters aim to store. We extracted 20 lexical features, including URL length, use of shortening services, and number of special characters, and used them to train a machine learning model. We divided the benign URLs into 80% as training data, 10% as validation data, and 10% as test data. All malicious URLs were used as training data and validation data.

**EMBER Dataset:** Following the previous studies on LBFs (Vaidya et al., 2021; Sato & Matsui, 2023), we used the EMBER dataset (Anderson & Roth, 2018). This dataset contains 400,000 malicious files and 400,000 benign files, their vectorized features, and sha256 hashes (the 200,000 unlabeled files were not used in our experiment). We used 10% of the benign files as training data, 10% as validation data, and 80% as test data. For the malicious files, 10% were used as training data, while all were used as validation data. This split ratio was adopted to avoid excessive training time due to the high dimensionality of the features in the EMBER dataset.

All experiments were implemented in C++ and conducted on a Linux machine equipped with an Intel® Core™ i9-11900H CPU @ 2.50 GHz and 64 GB of memory. The code was compiled using GCC version 11.4.0 with the `-O3` optimization flag, and all experiments were performed in single-threaded mode. Although any machine learning model can be used, we employed XGBoost (Chen & Guestrin, 2016), a widely used implementation of gradient boosting. Each weak learner in XGBoost corresponds to each machine learning model  $ML_1, \dots, ML_{\bar{D}}$  in our proposed method. The number of weak learners in XGBoost, i.e.,  $\bar{D}$ , is equal to `num_round`, a training parameter in XGBoost that specifies the number of boosting rounds. To clearly demonstrate the effectiveness of our CLBF, we have presented results from a straightforward comparison with a subset of the baseline methods. For more comprehensive experimental results, please refer to Appendices B to E.

#### 4.1. Memory and Accuracy

We compared the trade-off between memory usage and accuracy of CLBF with that of a standard Bloom filter and existing LBFs, specifically PLBF (Vaidya et al., 2021). Other baselines, such as sandwiched LBF (Mitzenmacher, 2018), are omitted here because they perform worse than PLBF in this trade-off. This trade-off is controlled by varying the hyperparameter  $F$  from 0.1 to 0.001. In this evaluation, we set  $\lambda = 1.0$ , meaning CLBF is optimized solely for memory efficiency. For CLBF, we set  $\bar{D}$ , i.e., the number of boosting rounds in XGBoost, to 100. For PLBF, we present results using XGBoost with boosting rounds  $D \in \{1, 10, 100\}$ , because PLBF lacks a mechanism for automatically adjusting

the model size.

Figure 4 presents the results. It shows that CLBF consistently achieves equal or better memory efficiency than the classic Bloom filter and PLBF, while CLBF does not need to evaluate different  $D$  values as PLBF does. In the Malicious URLs dataset, PLBF achieves optimal memory efficiency with  $D = 1$  or  $D = 10$ , and CLBF closely matches this efficiency. On the other hand, in the EMBER dataset, PLBF performs best with  $D = 10$  when  $F > 10^{-2}$  and with  $D = 100$  when  $F \leq 10^{-2}$ . Across all values of  $F$ , CLBF has better memory efficiency than PLBF. At  $F = 0.01$ , CLBF achieves a 24% reduction in memory usage compared to PLBF with  $D = 10$  and  $D = 100$ . These results indicate that the optimal model size  $D$  for achieving the best memory efficiency varies depending on both the dataset and the value of  $F$ , and that our CLBF can automatically select the optimal  $D$ .

#### 4.2. Memory and Reject Time

We compared the trade-off between memory usage and reject time in CLBF against existing LBFs and the standard Bloom filter. This trade-off in CLBF is controlled by varying the hyperparameter  $\lambda$  within the range  $[0, 1]$ . We set the false positive rate  $F$  for all methods to 0.001. The number of XGBoost boosting rounds (corresponding to  $\bar{D}$  in our method) was set to 100 for CLBF. Since the standard Bloom filter lacks a parameter to control this trade-off, it is represented as a point. For sandwiched LBF and PLBF, we observed the changes in memory usage and reject time when varying  $D$  from 1 to 100.

Figure 5 illustrates the results. We can see that CLBF greatly outperforms sandwiched LBF in terms of memory efficiency, and that CLBF greatly outperforms PLBF in terms of reject time. While the reject time of sandwiched LBF tends to be shorter than that of PLBF, its memory efficiency is inferior to both PLBF and CLBF. For example, in the EMBER dataset, CLBF achieves a minimum memory usage of approximately 400 kB, whereas no sandwiched LBF configuration uses less than 500 kB. On the other hand, although PLBF can achieve comparable memory efficiency to CLBF, it suffers from significantly longer reject times. Specifically, when the memory usage is around 500 kB in the EMBER dataset, the average reject time of CLBF is approximately 14 times shorter than that of PLBF.

Additionally, we can see that the CLBF plot forms a curve that is almost a Pareto front. In most cases, no other methods can achieve both lower memory usage and shorter reject time than CLBF. For CLBF itself, improving (or worsening) memory efficiency leads to a corresponding worsening (or improvement) in reject time. In contrast, for other LBFs, both the memory efficiency and reject time worsen as  $D$  becomes too large. Since it is impossible to know this

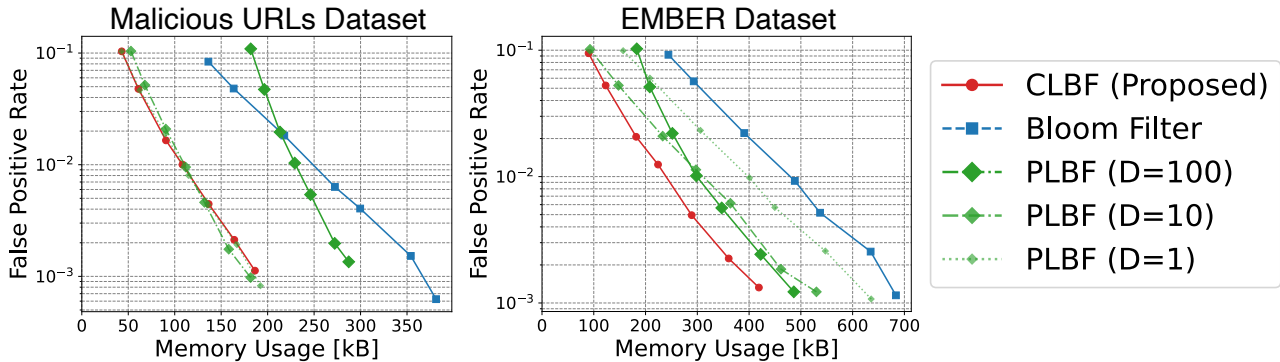


Figure 4: Trade-off between memory usage and accuracy (lower-left is better): CLBF achieves equal to or better memory efficiency than any other PLBF with  $D$ .

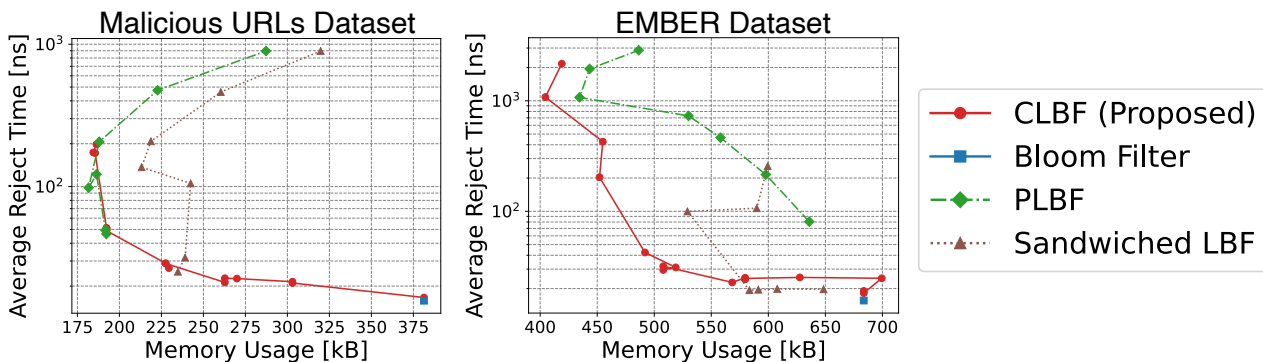


Figure 5: Trade-off between memory usage and average reject time (lower-left is better): Compared to PLBF with similar memory efficiency, CLBF achieves a significantly shorter average reject time (up to 14 times shorter).

turning point for  $D$  in advance, an imprudent choice of  $D$  risks constructing an LBF that is inefficient in terms of both memory and reject time. Our CLBF has the advantage of avoiding the risk of setting such a needlessly large  $D$ .

### 5. Limitations and Future Work

Our current optimization method does not always select the optimal intermediate layer thresholds, i.e.,  $\theta$ . While our experimental results demonstrate that selecting the best-performing thresholds from a set of candidates is sufficient to outperform existing LBFs in terms of memory efficiency and reject time, further improvements in threshold optimization could lead to even greater performance gains. Furthermore, while we currently discretize the false positive rates of Trunk Bloom filters, i.e.,  $f^{(t)}$ , at a certain granularity, future work could achieve better results by exploring more precise solutions.

Additionally, although our method is highly compatible with learning models composed of multiple weak learners, such as boosting, it cannot be directly applied to models com-

posed of a single large learner (e.g., a single deep learning model). To extend our approach for such models, it is necessary to introduce an additional mechanism that outputs tentative scores from intermediate layers. Here, a critical challenge is mitigating the memory and time overhead introduced by this mechanism. A novel optimization algorithm tailored to this framework may be required, and promising directions include leveraging advanced generic optimization techniques, such as Bayesian optimization or Adam.

### 6. Conclusion

In this research, we proposed CLBF, tackling two critical issues existing LBFs face. (1) By training a large machine learning model and reducing it optimally, CLBF achieves an optimal balance between model and filter sizes, minimizing overall memory usage. (2) By branching based on tentative scores and the insertion of intermediate Bloom filters, CLBF significantly reduces reject time. As a result, CLBF not only broadens the applicability of LBFs but also establishes a strong foundation for addressing these issues.



## Impact Statement

This paper presents work whose goal is to advance the field of Machine Learning. There are many potential societal consequences of our work, none which we feel must be specifically highlighted here.

## References

- Anderson, H. S. and Roth, P. Ember: An open dataset for training static pe malware machine learning models. *arXiv:1804.04637*, 2018.
- Bhattacharya, A., Gudes, C., Bagchi, A., and Bedathur, S. New wine in an old bottle: data-aware hash functions for bloom filters. *Proceedings of the VLDB Endowment*, 15(9):1924–1936, 2022a.
- Bhattacharya, A., Gudes, C., Bagchi, A., and Bedathur, S. Hash partitioned bloom filter (hpb). <https://github.com/data-iitd/PHBF/tree/main>, 2022b. Commit ID: e917150, accessed: 2024-11-20.
- Bloom, B. H. Space/time trade-offs in hash coding with allowable errors. *Communications of the ACM*, 13(7):422–426, 1970.
- Broder, A. and Mitzenmacher, M. Network applications of bloom filters: A survey. *Internet Mathematics*, 1(4):485–509, 2004.
- Chang, F., Dean, J., Ghemawat, S., Hsieh, W. C., Wallach, D. A., Burrows, M., Chandra, T., Fikes, A., and Gruber, R. E. Bigtable: A distributed storage system for structured data. *ACM Transactions on Computer Systems*, 26(2):1–26, 2008.
- Chen, T. and Guestrin, C. Xgboost: A scalable tree boosting system. In *ACM SIGKDD International Conference on Knowledge Discovery and Data Mining (KDD)*, 2016.
- Dai, Z. and Shrivastava, A. Adaptive learned bloom filter (ada-bf): Efficient utilization of the classifier with application to real-time information filtering on the web. In *Advances in Neural Information Processing Systems (NeurIPS)*, 2020.
- Dai, Z. and Shrivastava, A. Adaptive learned bloom filter (ada-bf): Efficient utilization of the classifier. <https://github.com/DAIZHENWEI/Ada-BF>, 2024. Commit ID: d6cf4ba, accessed: 2024-11-20.
- Dai, Z., Shrivastava, A., Reviriego, P., and Hernández, J. A. Optimizing learned bloom filters: How much should be learned? *IEEE Embedded Systems Letters*, 14(3):123–126, 2022.
- Dillinger, P. C. and Walzer, S. Ribbon filter: Practically smaller than bloom and xor. *arXiv:2103.02515*, 2021.
- Fan, B., Andersen, D. G., Kaminsky, M., and Mitzenmacher, M. D. Cuckoo filter: Practically better than bloom. In *ACM International Conference on Emerging Networking Experiments and Technologies (CoNEXT)*, 2014.
- Fumagalli, G., Raimondi, D., Giancarlo, R., Malchiodi, D., and Frasca, M. On the choice of general purpose classifiers in learned bloom filters: An initial analysis within basic filters. In *International Conference on Pattern Recognition Applications and Methods (ICPRAM)*, 2022.
- Geravand, S. and Ahmadi, M. Bloom filter applications in network security: A state-of-the-art survey. *Computer Networks*, 57(18):4047–4064, 2013.
- Goodrich, M. T. and Mitzenmacher, M. Invertible bloom lookup tables. In *Allerton Conference on Communication, Control, and Computing (Allerton)*, 2011.
- Graf, T. M. and Lemire, D. Xor filters: Faster and smaller than bloom and cuckoo filters. *Journal of Experimental Algorithmics*, 25:1–16, 2020.
- Kraska, T., Beutel, A., Chi, E. H., Dean, J., and Polyzotis, N. The case for learned index structures. In *ACM SIGMOD International Conference on Management of Data (SIGMOD)*, 2018.
- Lu, G., Nam, Y. J., and Du, D. H. Bloomstore: Bloom-filter based memory-efficient key-value store for indexing of data deduplication on flash. In *IEEE Symposium on Mass Storage Systems and Technologies (MSST)*, 2012.
- Malchiodi, D., Raimondi, D., Fumagalli, G., Giancarlo, R., and Frasca, M. The role of classifiers and data complexity in learned bloom filters: Insights and recommendations. *Journal of Big Data*, 11(1):1–26, 2024.
- Mitzenmacher, M. A model for learned bloom filters and optimizing by sandwiching. In *Advances in Neural Information Processing Systems (NeurIPS)*, 2018.
- Pagh, A., Pagh, R., and Rao, S. S. An optimal bloom filter replacement. In *ACM-SIAM Symposium on Discrete Algorithms (SODA)*, 2005.
- Sato, A. and Matsui, Y. Fast partitioned learned bloom filter. In *Advances in Neural Information Processing Systems (NeurIPS)*, 2023.
- Siddhartha, M. Malicious urls dataset. <https://www.kaggle.com/datasets/sid321axn/malicious-urls-dataset>, 2021. [Online; accessed 22-December-2022].
- Tarkoma, S., Rothenberg, C. E., and Lagerspetz, E. Theory and practice of bloom filters for distributed systems. *IEEE*

*Communications Surveys & Tutorials*, 14(1):131–155, 2011.

Vaidya, K., Knorr, E., Mitzenmacher, M., and Kraska, T. Partitioned learned bloom filters. In *International Conference on Learning Representations (ICLR)*, 2021.

Wang, M. and Zhou, M. Vacuum filters: More space-efficient and faster replacement for bloom and cuckoo filters. In *International Conference on Very Large Data Bases (VLDB)*, 2019.

Xie, R., Li, M., Miao, Z., Gu, R., Huang, H., Dai, H., and Chen, G. Icde-2021 - hash-adaptive-bloom-filter. <https://github.com/njulands/HashAdaptiveBF>, 2021a. Commit ID: 8add397, accessed: 2024-11-22.

Xie, R., Li, M., Miao, Z., Gu, R., Huang, H., Dai, H., and Chen, G. Hash adaptive bloom filter. In *International Conference on Data Engineering (ICDE)*, 2021b.

---

**Algorithm 1** Key Insertion into CLBF

---

```

1: Input: Key  $q$ 
2: Function: GetFBFIndex( $s$ ) returns the index of FBF corresponding to the score  $s$ .
3: for  $d = 1, 2, \dots, D$ 
4:   TBF $_d$ .Insert( $q$ )
5:    $s \leftarrow \text{ML}_d(q)$ 
6:   if  $d = D$  then
7:      $k \leftarrow \text{GetFBFIndex}(s)$ 
8:     FBF $_k$ .Insert( $q$ )
9:     break
10:  if  $s \geq \theta_d$  then
11:    BBF $_d$ .Insert( $q$ )
12:    break

```

---



---

**Algorithm 2** Query Processing in CLBF

---

```

1: Input: Query  $q$ 
2: Output: NotFound or Found
3: Function: GetFBFIndex( $s$ ) returns the index of FBF corresponding to the score  $s$ .
4: for  $d = 1, 2, \dots, D$ 
5:   if TBF $_d(q) = \text{NotFound}$  then
6:     return NotFound
7:    $s \leftarrow \text{ML}_d(q)$ 
8:   if  $d = D$  then
9:      $k \leftarrow \text{GetFBFIndex}(s)$ 
10:    return FBF $_k(q)$ 
11:  if  $s \geq \theta_d$  then
12:    return BBF $_d(q)$ 

```

---

## A. Algorithm Details

Here, we give a detailed description of the CLBF algorithm, which we omitted in the main text. First, in Appendix A.1, we explain the algorithm for inserting keys into CLBF and processing queries with CLBF, along with pseudocode. Then, in Appendix A.2, we describe the detailed algorithm for the dynamic programming method to determine the optimal configuration of CLBF.

### A.1. Algorithms for Key Insertion and Query Processing

The pseudocode for the algorithm that inserts keys into the CLBF is shown in Algorithm 1. First, the key  $q$  is inserted into the first Trunk Bloom filter, i.e., TBF $_1$ . Next, the output score from the first machine learning model, i.e., ML $_1$ , is obtained for the key  $q$ . If this score exceeds the threshold  $\theta_1$  corresponding to ML $_1$ , the algorithm branches to a Branch Bloom filter;  $q$  is inserted into BBF $_1$ , and the process terminates. Otherwise,  $q$  is passed to the next depth. If  $q$  does not branch into any Branch Bloom filters by the final depth  $d = D$ , it is inserted into the appropriate Final Bloom filter based on the final score. This process is repeated for all keys  $q$  contained in  $\mathcal{S}$ , the set stored by the CLBF.

Next, the pseudocode for the query algorithm in the CLBF is shown in Algorithm 2. Similar to key insertion, the query  $q$  is first checked against TBF $_1$ . If TBF $_1$  returns a NotFound result, it is certain that  $q \notin \mathcal{S}$ , and this result is returned immediately. Otherwise, the output score from ML $_1$  is obtained for  $q$ . If this score exceeds the threshold  $\theta_1$ , the algorithm branches to the Branch Bloom filter; the algorithm queries BBF $_1$  for  $q$ , and the result from this filter is used as the final result. Otherwise,  $q$  is passed to the next depth  $d$ . If  $q$  does not branch into any Branch Bloom filters by the final depth  $d = D$ , it is queried against the appropriate Final Bloom filter based on the final score. This approach leverages the tentative and final scores of the machine learning models to provide fast query responses while preserving the false-negative free property.

## A.2. Detailed Dynamic Programming Algorithm for Optimizing the CLBF Configuration

In this section, we explain the detailed dynamic programming algorithm for optimizing the CLBF configuration. As explained in the main text, our optimization method obtains the optimal CLBF configuration by recursively calculating the value of  $\text{dp}(d, T)$ , which is defined as the solution to the optimization problem (Equations (5) and (6)). The value of  $\text{dp}(d, T)$  is calculated recursively using the two functions  $\hat{\text{dp}}$  and  $\check{\text{dp}}$  as in Equation (9). In the following, we first explain in detail the method for calculating  $\hat{\text{dp}}$ , and then also explain how to calculate  $\check{\text{dp}}$ . Finally, we explain the implementation techniques and how they allow the computational complexity of this dynamic programming method to be  $\mathcal{O}(\bar{D}P^2 + \bar{D}PK)$ .

**The Method for Calculating  $\hat{\text{dp}}$ .**  $\hat{\text{dp}}(d, T)$  is the optimal solution for the case where the FBFs are placed directly under the  $\text{ML}_d$  (Figure 3a). In other words,  $\hat{\text{dp}}(d, T)$  is defined as the optimal solution of Equations (5) and (6) when the constraint  $D = d$  is added to the constraint. We determine the optimal  $f_d^{(t)}$  and  $\mathbf{f}^{(f)}$  by trying out several  $f_d^{(t)}$  values. For each fixed  $f_d^{(t)}$ , we determine the optimal  $\mathbf{f}^{(f)}$ , and then calculate the value of the objective function. In the following, we first explain how to determine the optimal  $\mathbf{f}^{(f)}$  for a fixed  $f_d^{(t)}$ , and then how to calculate the value of the objective function.

The important insight is as follows: For fixed  $T$  and  $f_d^{(t)}$ , the expected values of the proportions of keys and non-keys going into each  $\text{FBF}_k$  can be determined. For keys, this is exactly equal to  $g_{d,k}^{(f)}$ , since all keys pass the filtering by TBFs due to the false-negative free property. The expected proportion of non-keys entering  $\text{FBF}_k$  is  $h_{d,k}^{(f)}Tf_d^{(t)}$ , because non-keys can reach the final layer if and only if they pass all filtering by TBFs, whose false positives are  $\mathbf{f}^{(t)}$ . Since  $T = \prod_{j=1}^{d-1} f_j^{(t)}$ , the expected proportion of non-keys entering  $\text{FBF}_k$  is  $h_{d,k}^{(f)} \prod_{j=1}^d f_j^{(t)} = h_{d,k}^{(f)}Tf_d^{(t)}$ . Thus, for a fixed  $T$  and  $f_d^{(t)}$ , we can calculate the expected values of the proportions of keys and non-keys that enter each of the FBFs.

Using this insight, we can determine the optimal false positive rate for each  $\text{FBF}_k$ . We use the following insight from the PLBF paper (Vaidya et al., 2021): When the proportion of keys and non-keys entering a Bloom filter (for making the final decision) is  $g$  and  $h$ , respectively, we can minimize the overall memory usage by setting the false positive rate of this Bloom filter to be  $Fg/h$ , where  $F$  is the overall target false positive rate. Here, the term a Bloom filter for making the final decision refers to a Bloom filter such as BBF or FBF, whose output result becomes the overall answer for LBF. Following this insight, we can set the false positive rate of  $\text{FBF}_k$  to  $(Fg_{d,k}^{(f)})/(h_{d,k}^{(f)}Tf_d^{(t)})$ . Here, we define two functions,  $\tilde{f}(g, h)$  and  $\tilde{s}(g, \epsilon)$ , which we use to explain how to calculate the objective functions, as follows:

$$\tilde{f}(g, h) = \min\left(\frac{Fg}{h}, 1\right), \quad \tilde{s}(g, \epsilon) = cng \cdot \log_2\left(\frac{1}{\epsilon}\right). \quad (10)$$

In other words,  $\tilde{f}(g, h)$  represents the false positive rate that is set for FBF, where  $g$  and  $h$  are the expected proportions of keys and non-keys that are input to the Bloom filter, respectively.  $\tilde{s}(g, \epsilon)$  represents the memory usage of a Bloom filter with a false positive rate of  $\epsilon$  that holds  $n \cdot g$  keys. The constant  $c = \log_2(e)$  for the standard Bloom filter, and if a variant of the Bloom filter is used instead of the Bloom filter as TBFs, BBFs, and FBFs, then  $c$  will be a different value.

With the above insight, we can evaluate the value of the objective function (Equation (2)) because we can find the optimal  $\mathbf{f}^{(f)}$  for a fixed  $T$  and  $f_d^{(t)}$ . First, for the term  $M_d(D, \mathcal{F})$ , which is defined in Equation (7), we can express it as follows:

$$M_d(D, \mathcal{F}) = \text{Size}(\text{ML}_d) + \tilde{s}(g_d^{(t)}, f_d^{(t)}) + \sum_{k=1}^K \tilde{s}\left(g_{d,k}^{(f)}, \tilde{f}(g_{d,k}^{(f)}, h_{d,k}^{(f)}Tf_d^{(t)})\right). \quad (11)$$

We explain each term in Equation (11), while corresponding to each term in the definition (Equation (7)):

- The first term of Equation (7) is the first term of Equation (11) because  $D = d$ .
- The second term of Equation (7) is the second term of Equation (11) because  $D = d$ , the proportion of keys that go into  $\text{TBF}_d$  is  $g_d^{(t)}$ , and the false positive rate of the  $\text{TBF}_d$  is fixed at  $f_d^{(t)}$  now.
- The third term in Equation (7) is 0 because  $D = d$ .
- The fourth term in Equation (7) is the third term of Equation (11) because, as we explained earlier, we set the false positive rate of the  $\text{FBF}_k$  to be  $\tilde{f}(g_{d,k}^{(f)}, h_{d,k}^{(f)}Tf_d^{(t)})$ .

Second, for the term  $R_d(D, \mathcal{F})$ , which is defined in Equation (8), we can express it as follows:

$$R_d(D, \mathcal{F}) = \text{Time}(\text{ML}_d) \cdot h_d^{(t)} T f_d^{(t)}, \quad (12)$$

because  $D = d$  and  $\prod_{j=1}^d f_j^{(t)} = T f_d^{(t)}$ .

Following the above procedure, we can find the optimal  $\mathbf{f}^{(f)}$  for fixed  $T$  and  $f_d^{(t)}$ , and then compute the value of the corresponding value of the objective function. We compute the value of the objective function for each of the  $f_d^{(t)} \in \{p^0, p^1, \dots, p^{P-1}\}$ . Then we take the best of these results and set it as  $\hat{\text{dp}}(d, T)$ .

**The Method for Calculating  $\check{\text{dp}}$ .**  $\check{\text{dp}}(d, T)$  is the optimal solution for the case where the two-way branching is performed directly under the  $\text{ML}_d$  and the  $\text{TBF}_{d+1}$  and the  $\text{BBF}_d$  are arranged (Figure 3b). In other words,  $\check{\text{dp}}(d, T)$  is defined as the optimal solution of Equations (5) and (6) when the constraint  $D > d$  is added to the constraint. Similar to the case of  $\hat{\text{dp}}(d, T)$ , we determine the optimal configuration under the  $\text{ML}_d$  by trying out several  $f_d^{(t)}$  values. We calculate the objective function for each fixed  $f_d^{(t)}$ , and then choose the optimal one. In the following, we first explain how to determine the optimal configuration under the  $\text{ML}_d$ , and then how to calculate the value of the objective function.

First, the optimal false positive rate for  $\text{BFB}_d$  is  $\tilde{f}(g_d^{(b)}, h_d^{(b)} T f_d^{(t)})$ . This is because the expected proportions of keys and non-keys going into the  $\text{BFB}_d$  is  $g_d^{(b)}$  and  $h_d^{(b)} T f_d^{(t)}$ , respectively. Following the insight of PLBF, we can obtain that the optimal false positive rate of the  $\text{BFB}_d$  is  $\tilde{f}(g_d^{(b)}, h_d^{(b)} T f_d^{(t)})$ . In addition, for the configuration of  $\text{TBF}_{d+1}$  and below, the result of  $\text{dp}(d+1, T f_d^{(t)})$  can be used recursively. Here, note that  $\text{dp}(d+1, T f_d^{(t)})$  can be used because  $\prod_{j=1}^d f_j^{(t)} = T f_d^{(t)}$ .

Therefore, for a fixed  $f_d^{(t)}$ , the objective function in Equation (5) for the optimal configuration can be expressed as follows:

$$\frac{\lambda}{M_{\text{BF}}} \cdot \left\{ \tilde{s}(g_d^{(t)}, f_d^{(t)}) + \text{Size}(\text{ML}_d) + \tilde{s}\left(g_d^{(b)}, \tilde{f}(g_d^{(b)}, h_d^{(b)} T f_d^{(t)})\right) \right\} + \frac{1 - \lambda}{R_{\text{BF}}} \cdot h_d^{(t)} T f_d^{(t)} \cdot \text{Time}(\text{ML}_d) + \text{dp}(d+1, T f_d^{(t)}). \quad (13)$$

The first term is the (scaled) memory usage for  $\text{TBF}_d$ ,  $\text{ML}_d$ , and  $\text{BBF}_d$ . The second term is the (scaled) inference time for  $\text{ML}_d$ . The third term is the objective function (including memory usage and inference time) for  $\text{TBF}_{d+1}$  and below. By performing the above calculation for each fixed  $f_d^{(t)}$ , we can calculate the value of  $\check{\text{dp}}(d, T)$ .

**Implementation Techniques and Computational Complexity of Dynamic Programming.** With appropriate implementation, the computational complexity of this dynamic programming approach becomes  $\mathcal{O}(\bar{D}P^2 + \bar{D}PK)$ . Here, after explaining the computational complexity involved in a straightforward implementation, we describe the implementation tricks that reduce the computational complexity.

The number of possible values for  $d$ —the first argument of  $\text{dp}$ —is  $\bar{D}$ , and the number of possible values for  $T$ —the second argument of  $\text{dp}$ —is  $P$ . For each pair of  $d$  and  $T$ , up to  $P$  values of  $f_d^{(t)}$  are considered. The evaluation of  $\hat{\text{dp}}(d, T)$  takes  $\mathcal{O}(K)$  computational complexity, because the evaluation of  $M_d(D, \mathcal{F})$ , i.e., Equation (11), contains a summation from  $k = 1$  to  $k = K$ . Therefore, if we compute it naively, the total computational complexity of this dynamic programming is  $\mathcal{O}(\bar{D}P^2K)$ .

However, by reducing the complexity for evaluating  $M_d(D, \mathcal{F})$ , we can reduce the total computational complexity of this dynamic programming to  $\mathcal{O}(\bar{D}P^2 + \bar{D}PK)$ . By precomputing the summation in Equation (11) for each pair of  $d$  and “ $T f_d^{(t)}$ ,” we can evaluate this function in  $\mathcal{O}(1)$ . The time complexity of this precomputation is  $\mathcal{O}(\bar{D}PK)$ , because there are  $\bar{D}$  values for  $d$ ,  $P$  values for “ $T f_d^{(t)}$ ,” and  $\mathcal{O}(K)$  computations are required for each case. Therefore, the total computational complexity of this dynamic programming is  $\mathcal{O}(\bar{D}P^2 + \bar{D}PK)$ .

## B. Analysis of Model-Filter Memory Size Balance

Here, we experimentally show that our CLBF achieves an appropriate balance between model and filter size by appropriately reducing the given learned model. In order to clearly demonstrate the advantages of CLBF experimentally, we conduct experiments using a Random Dataset in addition to the two real-world datasets used in the main text:

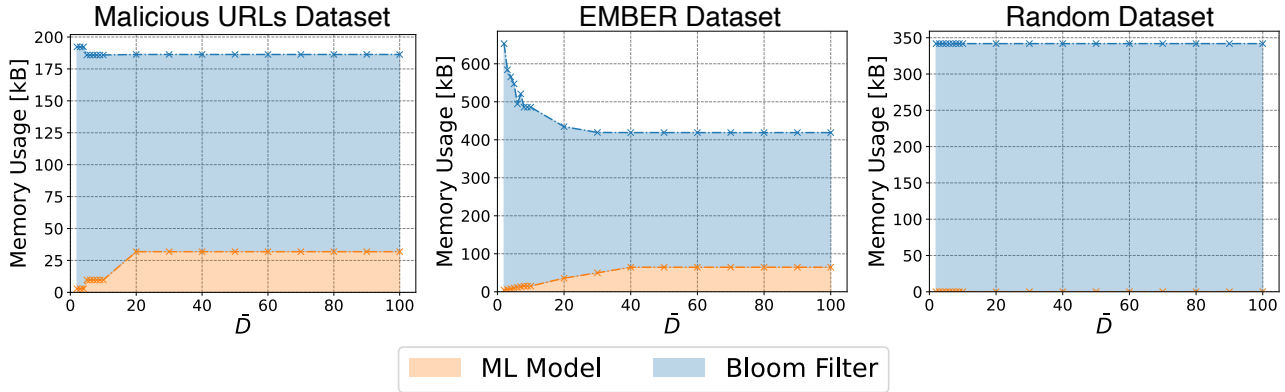


Figure 6: The model-filter memory size balance selected by CLBF for various  $\bar{D}$  values: Beyond a certain point, increasing  $\bar{D}$  further does not change the results.

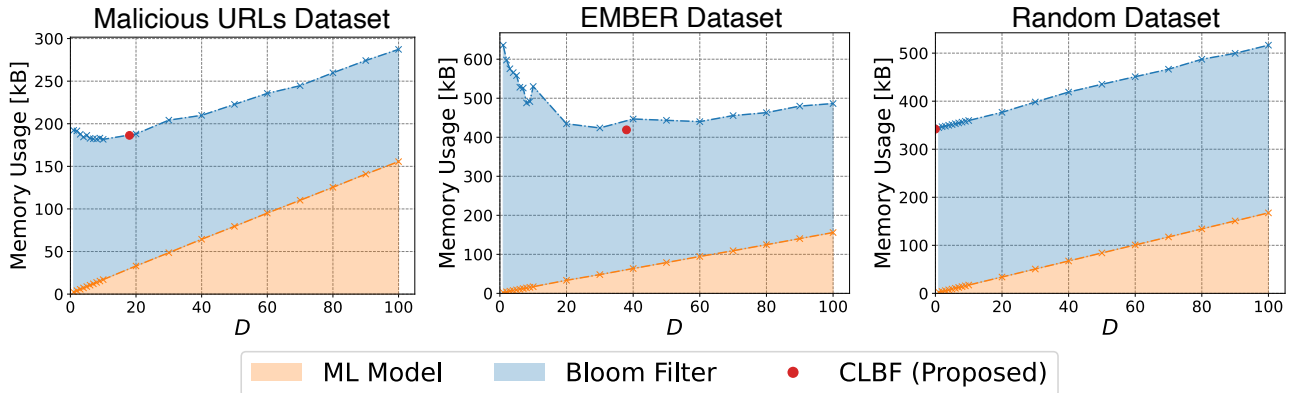


Figure 7: The model and filter memory size achieved by PLBF for various  $D$  values: Up to a certain point, increasing  $D$  reduces the overall memory usage, but beyond that point, increasing  $D$  starts to increase the overall memory usage.

**Random Dataset:** This dataset simulates a scenario where the distributions of key and non-key samples are identical, making it extremely challenging for a machine learning model to distinguish between them. The dataset is constructed as follows: We generate 700,000 20-dimensional feature vectors, where the values of each dimension are uniformly distributed between 0 and 1. Among these, 200,000 vectors are labeled as “key” and 500,000 as “non-key.” We divide the 500,000 non-key vectors into 80% as training data, 10% as validation data, and 10% as test data. All 200,000 key vectors are used as training data and validation data.

Figure 6 shows the relationship between the number of machine learning models given to construct CLBF, i.e.,  $\bar{D}$ , and the model-filter memory size balance chosen as a result of optimization (we always set  $F = 0.001$  here). When  $\bar{D}$  is small, increasing  $\bar{D}$  monotonically decreases the overall memory usage and monotonically increases the size of the machine learning models used. On the other hand, for a certain range of large values of  $\bar{D}$ , the size of the Bloom filter and the machine learning models used do not change because CLBF selects an optimal subset  $D$  from the given  $\bar{D}$  models. The optimal  $D$  varies by dataset: approximately 20 for the Malicious URLs dataset, 40 for the EMBER dataset, and 0 for the Random Dataset. This demonstrates that CLBF can efficiently reduce redundant models or avoid them entirely when they lack generalizability, as detected through validation data.

In contrast, in the case of PLBF (Vaidya et al., 2021), setting a larger  $D$  can lead to an increase in memory usage. The relationship between the number of machine learning models given when constructing PLBF, i.e.,  $D$ , and the memory usage of PLBF is shown in Figure 7 (we always set  $F = 0.001$  here). As  $D$  increases, of course, the memory usage of the PLBF machine learning models increases, because PLBF uses all of the  $D$  machine learning models given. On the other hand, the memory usage of the backup Bloom Filter used by PLBF tends to decrease. This is because the accuracy of the machine

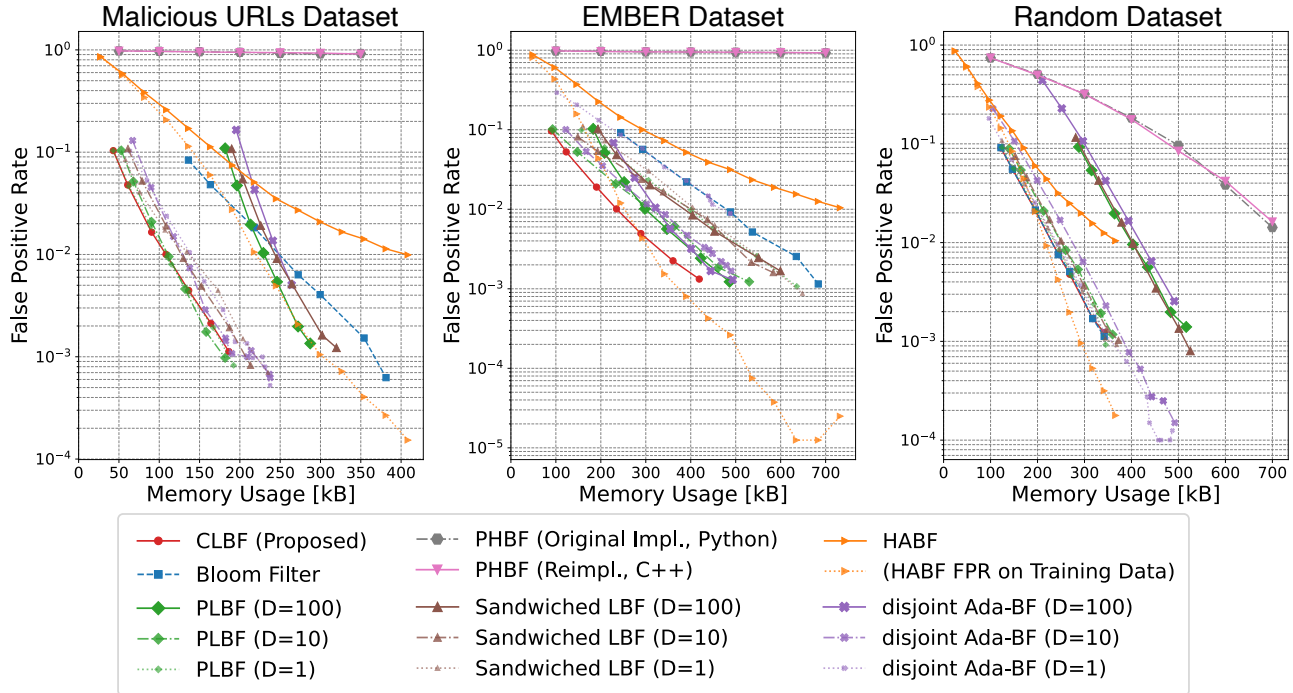


Figure 8: Trade-off between memory usage and accuracy (lower-left is better).

learning model tends to improve as the size of the machine learning model increases, and even a small Bloom Filter can achieve the target false positive rate. The overall memory usage decreases in the range of a certain small  $D$ , and increases in the range of a certain large  $D$ . The optimal  $D$  varies depending on the dataset, but in all cases, CLBF (shown as a red dot) selects a  $D$  close to the optimal value.

### C. Comparison Experiments with Other Baselines

Here, we present the comparison experiments with other baselines, which we omitted from the main text to avoid overly complicated result figures and to clearly demonstrate the effectiveness of our proposed method. In addition to the PLBF (Vaidya et al., 2021), the Sandwiched LBF (Mitzenmacher, 2018), and the Bloom filter (Bloom, 1970), we compare our CLBF with disjoint Ada-BF (Dai & Shrivastava, 2020) and Projection Hash Bloom Filter (PHBF) (Bhattacharya et al., 2022a), and Hash Adaptive Bloom Filter (HABF) (Xie et al., 2021b). We implemented the disjoint Ada-BF in C++ based on the Python implementation published by the authors (Dai & Shrivastava, 2024). For PHBF, we conducted experiments using both the Python implementation published by the authors (Bhattacharya et al., 2022b) and our own re-implementation in C++. The hyperparameter of PHBF, the sampling factor  $s$  is always set to 10, and the number of hash functions  $k$  is always set to 30. For HABF, we used the C++ implementation published by the authors (Xie et al., 2021a).

#### C.1. Memory and Accuracy

First, the trade-off between memory usage and accuracy for each method is shown in Figure 8. For CLBF, we always set  $\bar{D} = 100$ , and for PLBF, disjoint Ada-BF, and sandwiched LBF, we show the results for  $D = 1, 10, 100$ . For HABF, the results for  $\text{bits\_per\_key} = 1, 2, \dots, 15$  are shown. For HABF, the false positive rate in the training data is also displayed.

We can see that sandwiched LBF and disjoint Ada-BF always show inferior trade-offs compared to PLBF and CLBF with the same machine learning model size. In addition, the false positive rate for PHBF was always almost 1 for the Malicious URLs dataset and the EMBER dataset. This is thought to be because the mechanism of using the projection as a hash function results in false positives when there are keys in the set that have features similar to the non-key query. It is possible to improve the accuracy by increasing the PHBF hyperparameters  $k$ , i.e., the number of hashes, and  $s$ , i.e., the sampling

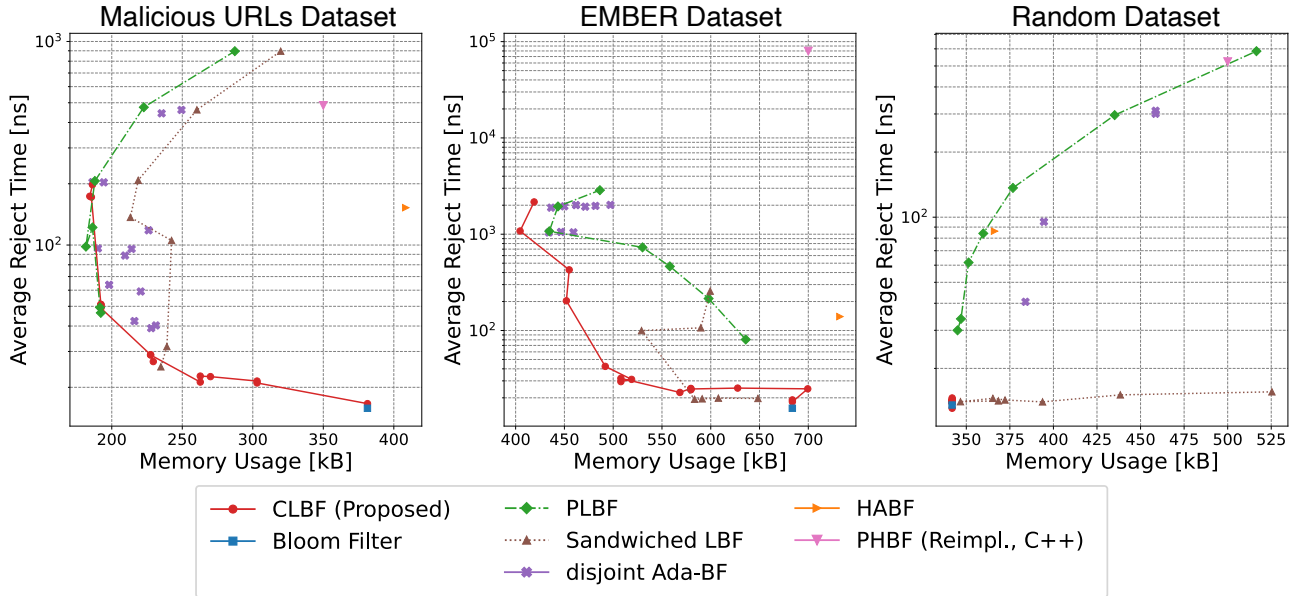


Figure 9: Trade-off between memory usage and average reject time (lower-left is better).

factor, but this will lead to an increase in construction time. Additionally, we observe that HABF has a worse accuracy than a simple Bloom filter. However, the HABF false positive rate for non-keys in the “training data,” i.e., the data used for optimization, is much better than the false positive rate for “test data.” In other words, HABF is found to be prone to overfitting. While HABF is effective in scenarios where the set of non-key queries is known at the time of construction, classic Bloom filters and LBFs achieve better accuracy in other cases.

### C.2. Memory and Reject Time

Next, the trade-off between memory usage and reject time for each method is shown in Figure 9. For PLBF, sandwiched LBF, and Bloom filter, we show the results for  $F = 0.001$ . Because the hyperparameter that controls the accuracy of disjoint Ada-BF is the total memory usage (instead of the target false positive rate, as in PLBF and CLBF), it is difficult to compare them under consistent conditions. Therefore, for disjoint Ada-BF, we constructed models with various total memory usages and  $D$ s, and then plotted only those with a false positive rate close to 0.001 (more precisely, greater than  $0.75 \times 0.001$  and less than  $1.25 \times 0.001$ ). For PHBF and HABF, we were unable to obtain a case with a sufficiently small false positive rate, so we have displayed the results for a case as a reference. Please note that it is **not** a fair comparison because the false positive rate is completely different between PHBF/HABF and other methods.

From Figure 9, we observe that our CLBF consistently achieves a shorter reject time than any of the baselines. For disjoint Ada-BF, when comparing with the same amount of memory usage, it was found that the reject time tended to be longer than PLBF. PHBF showed a long reject time compared to the other methods. In particular, the reject time of PHBF is particularly long for the EMBER dataset, which has a high dimensionality. This is because PHBF takes a long time to calculate the projection of the input vector.

### C.3. Construction Time

Finally, this section compares the time required to construct CLBF with other existing LBFs and the standard Bloom filter. The comparison is made with fast PLBF (Sato & Matsui, 2023), a method that constructs the same data structure as PLBF more quickly.

The results are shown in Figure 10. Here, “Scoring Time” refers to the time taken to measure the score of each sample against each machine learning model by passing validation data through them. “Configuration Time” refers to the time required to compute the optimal configuration using the results of the scoring phase. In the case of CLBF, the configuration process involves dynamic programming, as described in Section 3.3. Similarly, the configuration for sandwiched LBF and



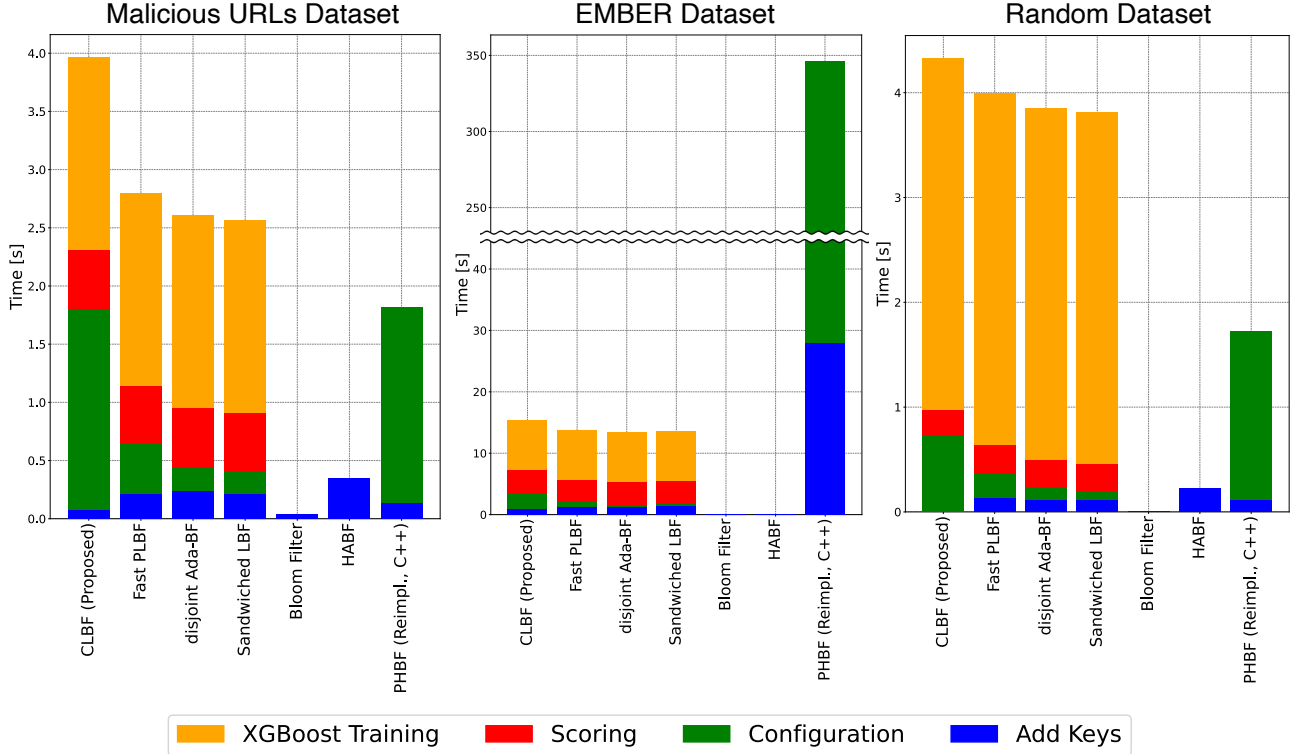


Figure 10: Construction time.

fast PLBF involves determining the optimal thresholds and false positive rates for each Bloom filter based on the scoring. For the LBFs (i.e., CLBF, PLBF, and sandwiched LBF), the input machine learning model size  $D = 100$ . For PLBF, sandwiched LBF, and Bloom filter, we show the results for  $F = 0.001$ . For disjoint Ada-BF, we show the results for total memory usage is 200 MB, and for HABF, we show for  $\text{bits\_per\_key} = 8$ .

The results indicate that CLBF requires a longer configuration time than other existing LBFs. The construction time of CLBF is approximately 10% to 40% longer than the construction time of existing LBFs. However, we believe that this additional overhead is a minor drawback. Considering that the construction time for the smallest sandwiched LBF is already about 100 times longer than that of a standard Bloom filter, we can assume that LBF is not something that is used in scenarios where construction speed is sensitive. LBFs should be used in contexts where the frequency of reconstruction is low (once an hour or less). For example, the (learned) Bloom filter used to filter malicious URLs does not need to be rebuilt frequently because the set of malicious URLs does not change that quickly. In such cases, the construction time of CLBF, which is 1.4 times longer than that of the sandwiched LBF, is not a problem, and the benefits of the optimal configuration obtained by searching virtually all cases of  $D \in \{1, 2, \dots, 100\}$  are considered to be greater.

We observe that the construction time for disjoint Ada-BF is almost identical to that of sandwiched LBF. This is because CLBF and PLBF use dynamic programming to find the optimal parameters, while disjoint Ada-BF uses heuristics to determine the parameters, similar to sandwiched LBF. The time required to build a PHBF is relatively short compared to LBFs, but the construction time is very long for the EMBER dataset, which has a high dimensionality.

The construction time of HABF is much shorter than that of the other LBFs. Although this speed is remarkable, as mentioned in Appendix C.1, HABFs tend to overfit, resulting in a higher false positive rate for unknown non-keys. On the other hand, LBFs achieve low false positive rates even for unknown non-keys, while taking longer time to construct. Therefore, LBFs and HABF are expected to be used in different application scenarios. Specifically, LBFs may be better suited for situations with less strict constraints on construction time (e.g., when the frequency of reconstruction is low), while HABF is more appropriate for scenarios where there are strict constraints on construction time and most of the non-key queries are known.

## D. Ablation Study on Hyperparameters of Machine Learning Models

CLBF obtains the optimal configuration by appropriately reducing the given trained machine learning model, but it is possible to further improve performance by appropriately tuning the machine learning model itself at the time of training. Here, we show the results of our observations on how the hyperparameters of the machine learning model XGBoost, in particular, the value of `max_depth`, affect the performance of LBF. The smaller the `max_depth`, the smaller each weak learner becomes, and while the size is smaller and inference time is shorter, the discriminative power of each weak learner becomes weaker.

The trade-off between memory usage and false positive rate for `max_depth` = 1, 2, 4, 6 is shown in Figure 11, and the trade-off between memory usage and reject time is shown in Figure 12, and the construction time is shown in Figure 13. We confirmed that the properties of CLBF, as shown in Section 4 and Appendix C, consistently appear for any value of `max_depth`: (1) better memory-accuracy trade-off than existing LBFs, (2) better memory-reject time trade-off than existing LBFs, (3) slightly (up to 1.8 times) longer construction time than existing LBFs.

We find that there is a performance range that cannot be achieved by either the CLBF method or hyperparameter tuning alone, i.e., there is a performance that can only be achieved by using both techniques. For example, in Figure 12, the performance of (Memory Usage, Reject Time) = (500 kB, 30 ns) can be achieved when `max_depth` = 4 and CLBF is used, but it cannot be achieved when `max_depth` = 1 or PLBF is used. These experimental results suggest the effectiveness of a hybrid method that combines the hyperparameter tuning of the machine learning model and the optimization technique in CLBF.

## E. Experimental Analysis on Artificial Datasets with Different Levels of Learning Difficulty

Here, we experimentally demonstrate that CLBF can adaptively select an appropriate machine learning model size based on the learning difficulty of the dataset. We generate synthetic datasets with different levels of learning difficulty using two distinct methods. Each dataset consists of 200,000 keys and 500,000 non-keys. Each key and non-key is represented by a 20-dimensional feature vector, generated according to the following procedures:

**Separation-Controlled Dataset.** This dataset is constructed to control the ease of learning by adjusting the parameter  $\delta$ , which determines the separation between the distributions of keys and non-keys. Each feature vector is generated as follows:

- The key feature vectors are sampled from a normal distribution  $\mathcal{N}(\mathbf{0}, I)$ , where  $\mathbf{0}$  is a 20-dimensional vector filled with zeros and  $I$  is the  $20 \times 20$  identity matrix.
- The non-key feature vectors are sampled from a normal distribution  $\mathcal{N}(\delta\mathbf{1}, I)$ , where  $\mathbf{1}$  is a 20-dimensional vector filled with ones.

As  $\delta$  increases, the distributions of keys and non-keys become more separated, making it easier for a machine learning model to distinguish between them. Conversely, a smaller  $\delta$  makes the distributions overlap, increasing the difficulty of learning. Figure 14 shows the Separation-Controlled Dataset for the 2-dimensional case with  $\delta = 0.0, 2.5, 5.0$ . The larger the value of  $\delta$ , the more the key and non-key distributions are separated, and the easier it is for the machine learning model to distinguish between keys and non-keys.

**Cluster-Number-Controlled Dataset.** This dataset is designed to control the learning complexity by varying the parameter  $c$ , which specifies the number of clusters formed by the key and non-key feature vectors. Each feature vector is generated as follows:

- The cluster centers for keys ( $\{\mathbf{p}_i\}_{i=1}^c$ ) and non-keys ( $\{\mathbf{q}_i\}_{i=1}^c$ ) are independently sampled from a uniform distribution over  $[-10, 10]$ .
- The key feature vectors are sampled equally from  $\mathcal{N}(\mathbf{p}_1, I), \mathcal{N}(\mathbf{p}_2, I), \dots, \mathcal{N}(\mathbf{p}_c, I)$ .
- Similarly, the non-key feature vectors are sampled equally from  $\mathcal{N}(\mathbf{q}_1, I), \mathcal{N}(\mathbf{q}_2, I), \dots, \mathcal{N}(\mathbf{q}_c, I)$ .

When  $c$  is small, the distributions form a few well-separated clusters, making the classification task easier. Conversely, as  $c$  increases, the clusters become more numerous, resulting in greater overlap and increased learning difficulty. Figure 15

shows the Cluster-Number-Controlled Dataset for the 2-dimensional case with  $c = 1, 8, 64$ . The larger the value of  $c$ , the more complex the distribution of key and non-key data becomes, and the more difficult it is for the machine learning model to distinguish between keys and non-keys.

By measuring the memory usage of CLBF and PLBF for various values of  $\delta$  and  $c$ , we confirm that CLBF dynamically adjusts its model size based on the dataset’s learnability. Figure 16 shows the memory usage of CLBF and baselines in the Separation-Controlled Dataset ( $\delta = 0, 0.5, 1.0, 1.5, \dots, 5.0$ ) and the Cluster-Number-Controlled Dataset ( $c = 1, 2, 4, 8, \dots, 16384$ ). The false positive rate  $F$  is always set to 0.001 here.

First, in the Separation-Controlled Dataset, we observe that the appropriate size of the machine learning model differs depending on the value of  $\delta$ , and that CLBF effectively selects the optimal size at all times. When  $\delta$  is very small ( $\delta \sim 0.0$ ), it is optimal not to use a machine learning model ( $D = 0$ ). However, PLBF retains unnecessary machine learning models, making it less memory efficient than a classical Bloom filter. For  $\delta$  values between 0.5 to 1.0, it is optimal to use a medium-sized machine learning model ( $D \sim 20$ ). As we increase the value of  $\delta$  further, the optimal  $D$  decreases, and when  $\delta = 5.0$ , it is optimal to use a very small machine learning model ( $D = 1$ ). Across all these scenarios, CLBF consistently selects the optimal model size, achieving lower memory consumption than all baselines.

Similarly, results from the Cluster-Number-Controlled Dataset also demonstrate the effectiveness of CLBF. When  $c$  is very large ( $c \geq 10^3$ ), it is optimal not to use a machine learning model ( $D = 0$ ), whereas PLBF retains redundant models, leading to inefficiencies compared to a classical Bloom filter. For  $10^2 \leq c < 10^3$ , it is optimal to use a medium-sized machine learning model ( $D \sim 50$ ). As we decrease the value of  $c$  further, the optimal  $D$  decreases, and when  $c = 1$ , it is optimal to use a very small machine learning model ( $D = 1$ ). In all cases, CLBF successfully adapts its model size and consistently achieves lower memory usage than the baselines.

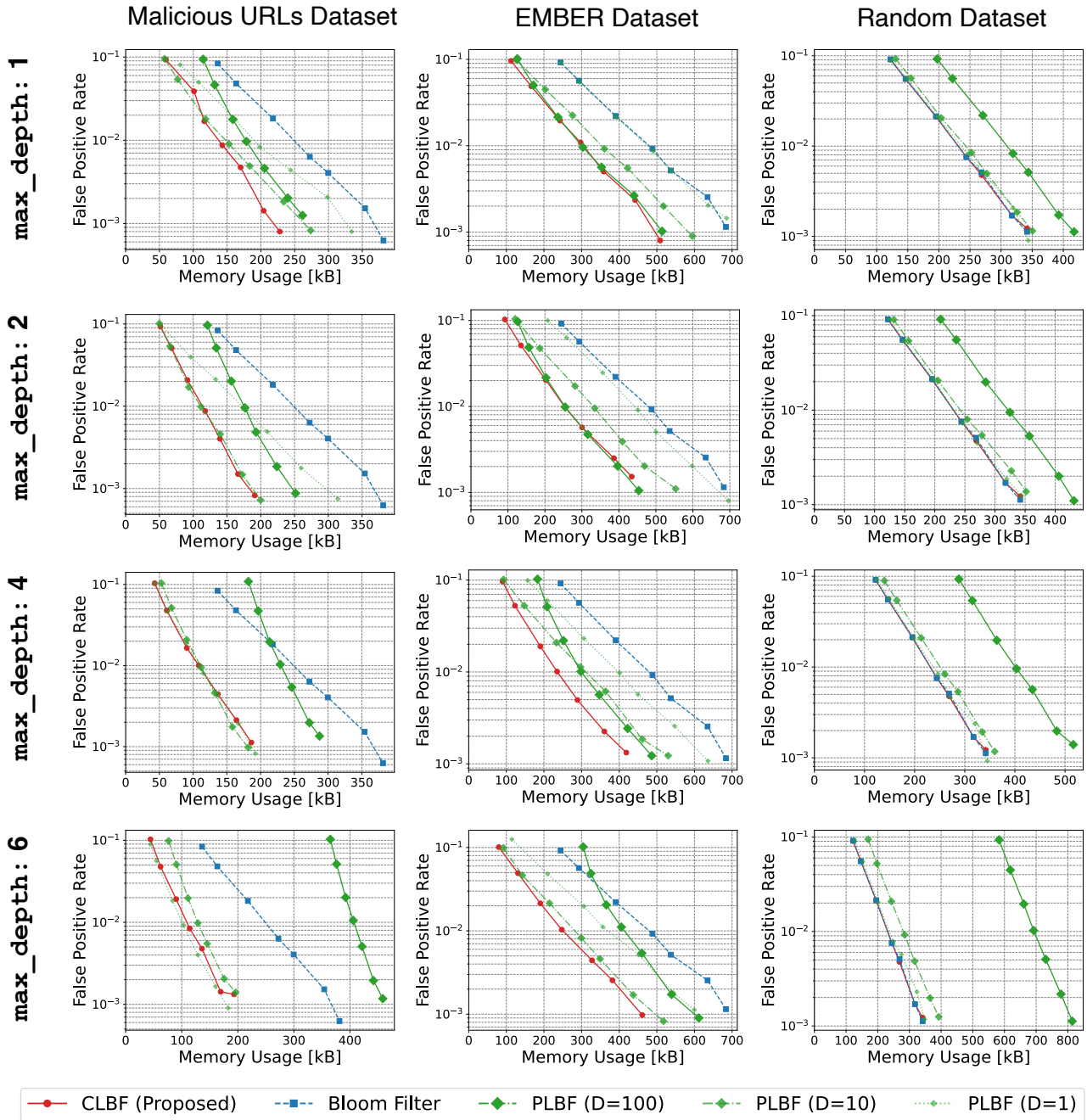


Figure 11: Trade-off between memory usage and accuracy (lower-left is better).

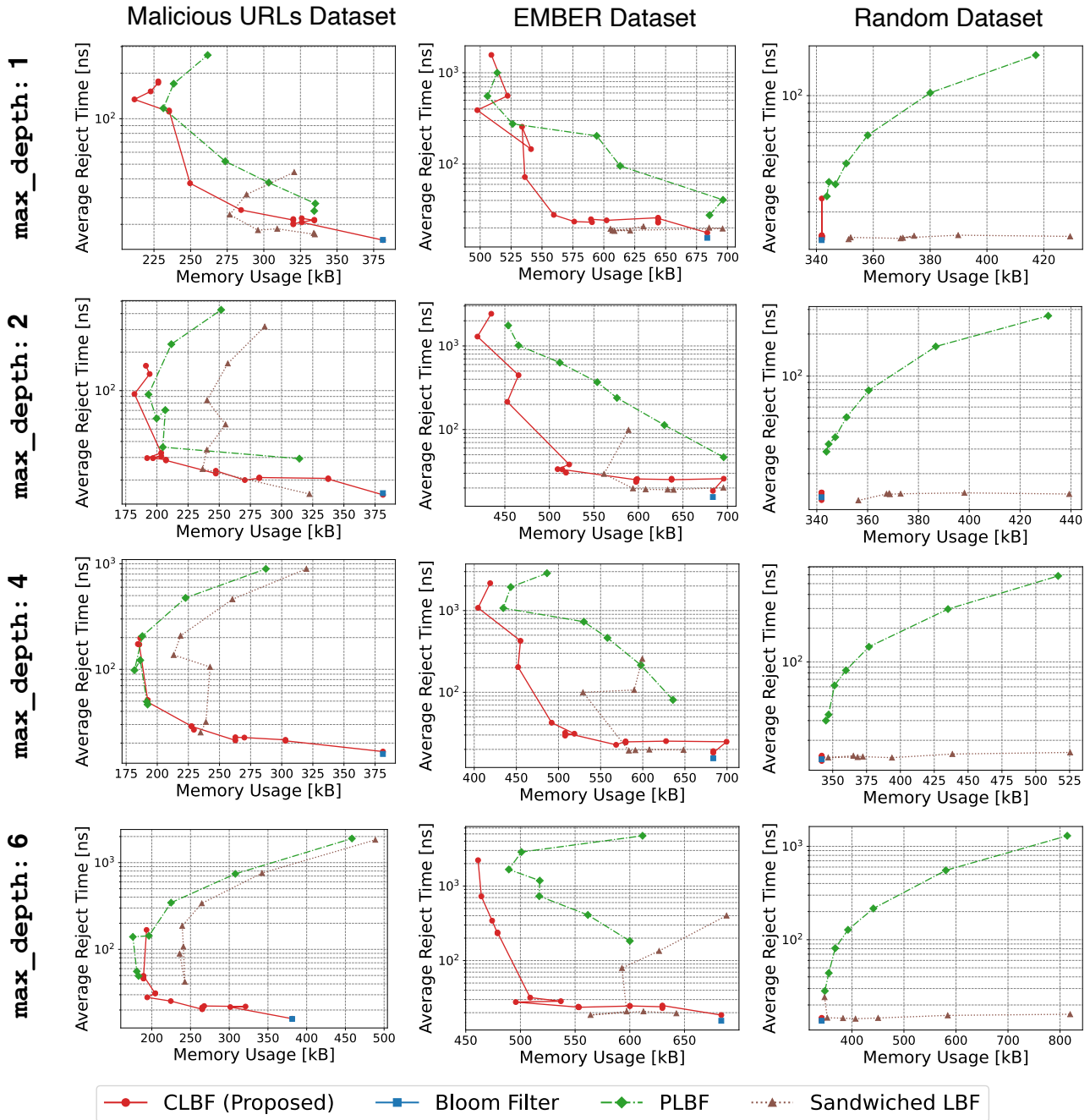


Figure 12: Trade-off between memory usage and average reject time (lower-left is better).

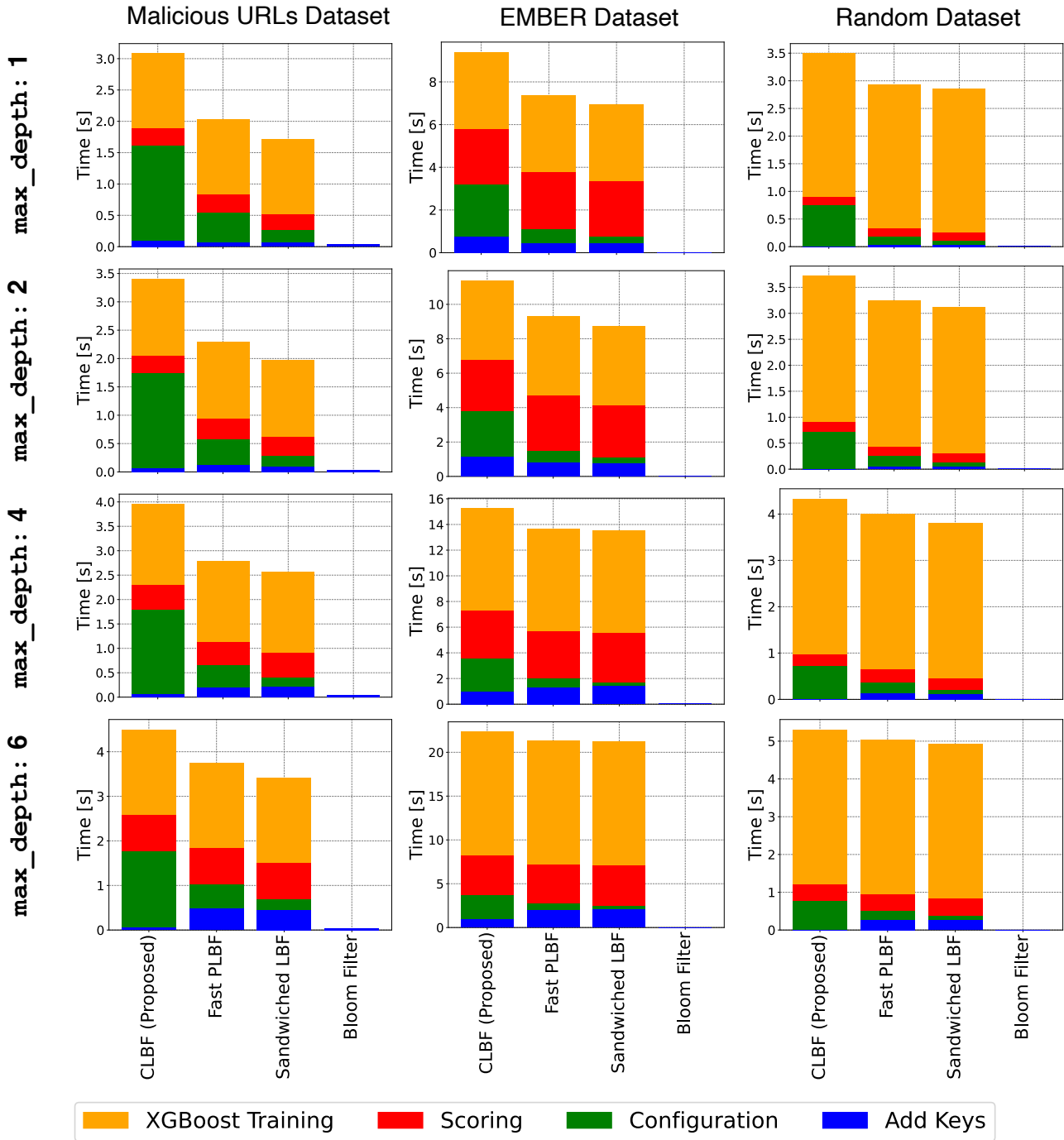


Figure 13: Construction time.

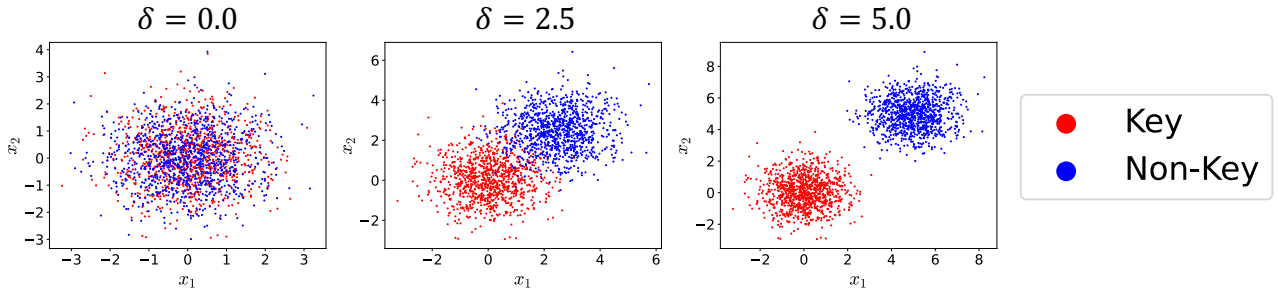


Figure 14: Visualization of Separation-Controlled Dataset in 2D.

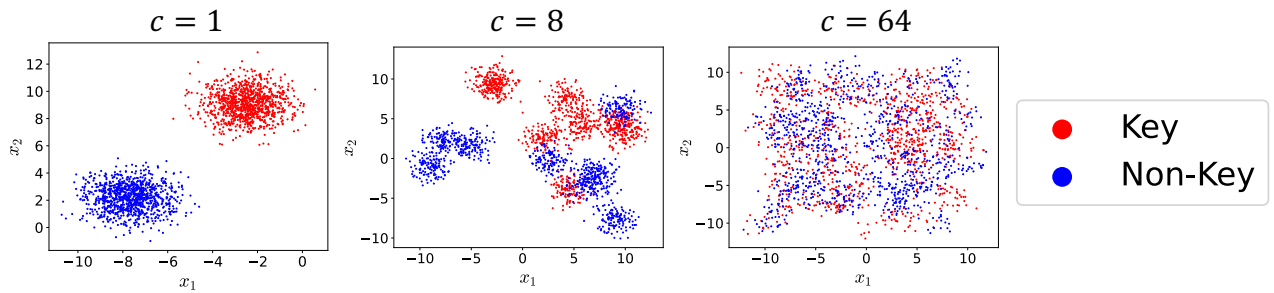


Figure 15: Visualization of Cluster-Number-Controlled Dataset in 2D.

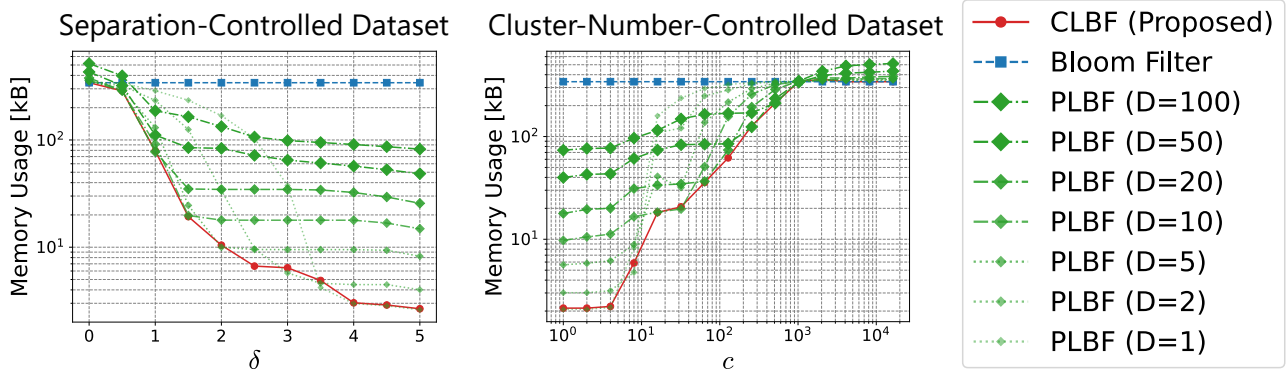


Figure 16: Memory usage of CLBF and baselines in the Separation-Controlled Dataset with various values of  $\delta$  and the Cluster-Number-Controlled Dataset with various values of  $c$ .